SANDIA REPORT

SAND2006-1789
Unlimited Release
Printed March 2006

Model Reduction of Systems with Localized Nonlinearities

Daniel J. Segalman

Prepared by
Sandia National Laboratories
Albuquerque, New Mexico 87185 and Livermore, California 94550

Sandia is a multiprogram laboratory operated by Sandia Corporation,
a Lockheed Martin Company, for the United States Department of Energy's
National Nuclear Security Administration under Contract DE-AC04-94-AL85000.

Issued by Sandia National Laboratories, operated for the United States Department of Energy by Sandia Corporation.

Available to DOE and DOE contractors from
U.S. Department of Energy
Office of Scientific and Technical Information
P.O. Box 62
Oak Ridge, TN 37831

Telephone: (865) 576-8401
Facsimile: (865) 576-5728
E-Mail: reports@adonis.osti.gov
Online ordering: http://www.doe.gov/bridge

Available to the public from
U.S. Department of Commerce
National Technical Information Service
5285 Port Royal Rd
Springfield, VA 22161

Telephone: (800) 553-6847
Facsimile: (703) 605-6900
E-Mail: orders@ntis.fedworld.gov
Online ordering: http://www.ntis.gov/ordering.htm

SAND2006-1789
Unlimited Release
Printed March 2006

Model Reduction of Systems with Localized Nonlinearities

Daniel Segalman
Structural Dynamics Research Department
Sandia National Laboratories
P.O. Box 5800
Albuquerque, NM 87185-0557
djsegal@sandia.gov

Abstract

An LDRD funded approach to development of reduced order models for systems with local nonlinearities is presented. This method is particularly useful for problems of structural dynamics, but has potential application in other fields. The key elements of this approach are 1) employment of eigen modes of a reference linear system, 2) incorporation of basis functions with an appropriate discontinuity at the location of the nonlinearity.

Galerkin solution using the above combination of basis functions appears to capture the dynamics of the system with a small basis set. For problems involving small amplitude dynamics, the addition of discontinuous (joint) modes appears to capture the nonlinear mechanics correctly while preserving the modal form of the predictions. For problems involving large amplitude dynamics of realistic joint models (macro-slip), the use of appropriate joint modes along with sufficient basis eigen modes to capture the frequencies of the system greatly enhances convergence, though the modal nature the result is lost.

Also observed is that when joint modes are used in conjunction with a small number of elastic eigen modes in problems of macro-slip of realistic joint models, the resulting predictions are very similar to those of the full solution when seen through a low pass filter. This has significance both in terms of greatly reducing the number of degrees of freedom of the problem and in terms of facilitating the use of much larger time steps.

Acknowledgment

The author thanks Thomas Burton of New Mexico State University for alerting the author to the papers of Milman and Chu as well as for several helpful suggestions for exploration of the methods presented here. Thanks are also due to the author's colleagues Todd Griffith, James Lauffer, Garth Reese, and Matt Hoplins at Sandia National Laboratories for reviewing versions of this report and making many helpful suggestions.

Contents

1 Introduction **7**

2 Formulation **9**

Galerkin formulation for a System of Localized Nonlinearity 9

Reference Linear System 10

Galerkin Solution, Modal Truncation, and Slightly Nonlinear Systems 11

Problems of Larger Nonlinearity 11

Joint Modes 12

Eigen Vector Sensitivities 12

Milman-Chu Modes 13

3 Model Reduction for a Structure Containing a Mechanical Joint **15**

Whole-Joint Approximation 16

The Four-Parameter Iwan Model 16

Numerical Results for Problems of Micro-Slip 17

Numerical Results for Problems of Macro-Slip 18

4 Implementation in the Context of Finite Element Analysis **21**

Automatic Determination of Special Vectors and Matrices 21

Algebraic Vector F_j 21

Gradient Matrix K_N 22

Milman-Chu Algebraic Vector $y_{MC,j}$ 22
Employment in Conjunction with Component Mode Synthesis 22
How Many Modes? 23

5 Conclusion **25**

References **31**

Model Reduction of Systems with Localized Nonlinearities

Chapter 1

Introduction

Though the weapons program has access to massively parallel computers and has finite element code that can employ many processors simultaneously, the resulting numerical predictions often are difficult to interpret physically. This difficulty is particularly frustrating in the area of structural dynamics where modal analysis has historically been a major tool both for calculation and for interpretation. Once the nonlinearity of the structure has been acknowledged, modal analysis no longer applies and the remaining tools are awkward to apply and without intuitively obvious physical meaning. The need to address this issue motivated the LDRD funding that made the work discussed in the following possible.

The method presented here provides a partial resurrection of modal analysis in the context of nonlinear structures whose nonlinearity is local in nature. Though for problems of large size or complexity it is still be necessary to employ large computing resources in order to exploit the method presented here, two major advantages are gained:

1. The results are presented in terms of modal coordinates so that often the predictions lend themselves to direct physical interpretation.

2. The reduced order system runs so quickly that many calculations over long periods of time can be run casually. Force boundary conditions can be changed and the system can be recalculated with minimal difficulty or additional computer resources.

The most straight-forward approach to model reduction for nonlinear systems is that of employing assumed modes in a Galerkin formulation. (A good discussion on Galerkin methods can be found in [5].) This is the approach most often used in problems of modest and diffuse nonlinearity and it is often very successful. As one would expect, the success of a Galerkin approach depends largely on whether the set of basis functions employed span the space of the full solution. We shall see that in cases of localized nonlinearities, it is

necessary to include within the basis functions ones that can accommodate the locality of the nonlinearity. Examples are provided.

The initial portion of this report employs mathematical quantities specific to interfaces. How one evaluates those quantities is discussed in a following section.The presentation that follows focuses specifically on problems of structural dynamics, but one anticipates that these techniques could be applied to model reduction of other classes of problem characterized by local nonlinearity.

Chapter 2

Formulation

Galerkin formulation for a System of Localized Nonlinearity

Here we assume a discretization has already been performed - probably by a fine level Galerkin finite element process. The governing equation now has the following nonlinear differential-algebraic form:

$$M\ddot{u} + C\dot{u} + \hat{K}u + \sum_j f_j(s_j, \{\zeta_j\})F^j = f_x(t) \tag{2.1}$$

Above M is the mass matrix and C is the damping matrix, the f_j are (nonlinear) forces acting between node pair j of the system and f_x is the vector of external loads. The nonlinear interface force f_j is a function of the distance s_j between node pair j and of state variables $\{\zeta_j\}$ that evolve along with s_j. The matrix $\hat{K}$ captures the linear elasticity of the rest of the structure; it is the stiffness matrix of a conventional finite element code, where the nonlinear interfaces are ignored.

The vector F^j captures the direction of forces between the node pair j (system degrees of freedom j_1 and j_2) and is related to nodal kinematics by

$$F_k^j = \partial s_j / \partial u_k \tag{2.2}$$

where u_k is the k^{th} degree of freedom of the finite element discretization.

The Galerkin procedure begins with some assumed deformation modes $\{y_k\}$ so that the kinematics of the problem can be approximated by

$$u(t) = a_k(t) y_k \tag{2.3}$$

The coefficients $\{a_k(t)\}$ are referred to as generalized coordinates. Here and in the following, summation on repeated indices is assumed.

The next step is to assert that the residual is orthogonal to the each of the assumed deformation modes:

$$y_n^T M y_k \ddot{a}_k + y_n^T C y_k \dot{a}_k + y_n^T \hat{K} y_k a_k + f_j(s_j, \{\zeta_j\}) y_n^T F^j = y_n^T f_x(t) \tag{2.4}$$

for each y_n. This is simplified as

$$\tilde{M}\ddot{a} + \tilde{C}\dot{a} + \tilde{K}a + f_j(s_j, \{\zeta_j\})\tilde{F}^j = \tilde{f}_x(t) \tag{2.5}$$

Ideally, one can obtain adequate solutions to the nonlinear system with far fewer basis functions y_n than the degrees of freedom of the original finite element formulation. The success of a Galerkin approach generally hinges on the appropriate choice of basis functions.

Reference Linear System

The first basis functions that come to mind are the eigen modes of a reference linear system.

Say that at small loads, our interface forces can be approximated as

$$d f_j(s_j, \{\zeta_j\}) = \left.\frac{\partial f_j(s, \{\zeta_j = 0\})}{\partial s}\right|_{s=0} ds_j = k_j \, ds = k_j F^j \, du \tag{2.6}$$

In that range of small loads, the governing equation (Eq. 2.1) becomes

$$M\ddot{u} + C\dot{u} + K_0 u = f_x(t) \tag{2.7}$$

where

$$K_0 = \hat{K} + \sum_j k_j F^j F^{j^T} \tag{2.8}$$

The use of a subset of the eigen modes of the reference linear system (RLS) in the linear system itself is the familiar modal truncation. Modal truncation of a RLS is illustrated on the structure depicted in Figure 1. The eleven unit masses of this system are connected by springs of unit stiffness. An external triangularly shaped impulse of duration equal to one quarter of the longest period is applied to the mass at the free end. It is primarily the first mode that is excited, so one expects modal truncation to serve as a good approximation to the full system. Indeed Figure 2 shows modal truncation to be quite adequate for this problem. In this figure and in other kinetic energy plots, the legend refers to the envelopes of the kinetic energies.

Galerkin Solution, Modal Truncation, and Slightly Nonlinear Systems

Let's now consider a system that is just slightly nonlinear. We supplement the unit spring between the 5^{th} and 6^{th} masses of the structure in Figure 1 with a slightly nonlinear spring so that the net force between the masses is

$$f(s) = K_1 s + K_2 s^3 \tag{2.9}$$

where $K_1 = 1$ and $K_2 = 50$. This structure is shown symbolically in Figure 3. Here we consider a very low amplitude (peak force $F_0 = 0.05$) externally applied impulse so that only a little of the nonlinearity is manifest (see Figure 4 for the force displacement plot.). Here the full solution of the nonlinear system of eleven differential algebraic equations is our truth model.

We use eigen modes of the reference linear system as basis functions in the Galerkin formulation. Examination of the kinetic energies predicted by our truth model and the reduced models are shown in Figure 5. The good agreement between the predicted kinetic energies argues that for this case, a Galerkin procedure using eigen modes of a RLS can yield good approximation.

Another indication of the adequacy of the RLS modes to capture the response of the slightly nonlinear system is a comparison of the singular value decomposition (SVD) modes of the solution of the full nonlinear system with the RLS eigen modes. (A good discussion on using SVD to explore the properties of nonlinear systems can be found in [6].) Figure 6 shows the first SVD mode and the first RLS eigen mode to be nearly identical. Figure 7 shows that it is only the first SVD mode that plays a significant role in the response to the low amplitude triangular impulse.

Problems of Larger Nonlinearity

Problems of even large nonlinearity are often quite amendable to Galerkin approximation employing modes of neighboring linear systems. Generally those successes are ones where the nonlinearity is diffused smoothly through a significant part of the structure. We show in this section examples of problems where the nonlinearity is very local in nature and the eigen modes of a reference linear system are a less adequate basis.

Consider an eleven-element nonlinear structure identical to that discussed above (Figure 3), but subject to a higher amplitude triangular impulse. The force-displacement curve of the parallel linear and cubic springs is shown in Figure 8 where significant nonlinearity is observed.

This problem is much less amenable to Galerkin solution using the RLS eigen modes. Figure 9 shows the kinetic energy of the system over time predicted by the full nonlinear solution and by various levels of Galerkin approximation. Not only is approximation by five modes inadequate, but approximation by even ten modes results in significant error. Only when the number of modes is equal to the total number of physical degrees of freedom of the system does the kinetic energy predicted by a modal approximation match that of the full nonlinear solution.

The source of the difficulty of performing model reduction of systems of local nonlinearity is suggested in Figure 10 where the first SVD mode of the full nonlinear solution and the first eigen mode of the RLS are shown. We see an apparent discontinuity in the SVD mode. Because there is a stiffening spring between the 5^{th} and 6^{th} masses, there is less deformation there than in the corresponding mode of the RLS. One should not be surprised that attempting to capture this apparent discontinuity with a sum of modes of the RLS would result in a Gibbs' type phenomenon requiring a very large number of modes.

Joint Modes

One anticipates that discontinuities such as that illustrated in the SVD mode of the above problem will be characteristic of systems with local stiffness nonlinearities. So one should expect to encounter convergence issues when using approximation by modes of a reference linear system. One well-known approach to accommodating analogous problems in Fourier analysis is to subtract out the discontinuity; that is to augment the basis functions with a simple function sharing the discontinuity of the function to be approximated.

Two candidate classes of basis function were examined for this study. The first is one associated with eigen vector sensitivity analysis and the second is one associated with the static response of the RLS to self-equilibrating loads.

Eigen Vector Sensitivities

The term eigen vector sensitivity can mean the sensitivity of eigen vectors of a matrix system to small perturbations of those matrices or it may refer to sensitivities of the eigenvectors of a mechanical system to physical parameters of that system. The concepts presented here fit into both categories.

Consider a mechanical system with a nonlinear but differentiable connection between degrees of freedom x_{J_1} and x_{J_2} and that the tangent stiffness at zero load of that connection is k_J. As before, the stiffness matrix for that reference linear system is K_0 and the mass matrix is M. We select an eigen mode, V_m^J, of the reference linear system that causes significant deformation at connection J.

Consider also another linear system that differs from the reference linear system only in the stiffness at connection J, where the stiffness is $k_J + \delta k_J$. The m^{th} eigen mode of this perturbed system is $V_m^J + \delta V_m^J$ and the sensitivity of the m^{th} eigen mode with respect to stiffness at the connection is

$$\hat{V}_m^J = \delta V_m^J / \delta k_J \tag{2.10}$$

Because the eigenvectors of the perturbed systems differ from those of the reference system primarily in the displacement across the connection, sensitivity vectors will manifest a discontinuity at the connection location. The reasoning presented above to explain the slow convergence of a Galerkin procedure using only the eigen modes of the RLS would argue that the discontinuity found in these perturbed eigen modes could make them valuable in accelerating the convergence of the Galerkin process. The sensitivity of the first eigen mode of our example system with respect to the stiffness of the connection between the 5^{th} and 6^{th} masses is shown in Figure 11.

The strategy proposed above is illustrated in Figure 12. Here we see that a Galerkin basis that consists of the first four eigen modes of the RLS and the sensitivity mode presented in Figure 11 almost exactly captures the kinetic energy predicted by the full nonlinear solution. In fact, even the use of just one eigen mode along with the sensitivity mode does a pretty good job of predicting the kinetic energy (Figure 13).

Milman-Chu Modes

In addressing the optimal selection of dampers for linear systems, Milman and Chu ([1], [8])introduced basis functions obtained by solving the statics problem of self-equilibrating loads acting between the degrees of freedom where the linear damper was intended. A character of these basis functions is that they have a discontinuity at the location of that connection.

Milman and Chu referred to their basis functions as Ritz vectors. Because this term is so general as to be unhelpful in the context of the work reported here, we refer to their basis functions as Milman-Chu vectors.

The Milman-Chu vector for our reference linear system is shown in Figure 14, where that anticipated discontinuity is manifest. In Figures 15 and 16 we see that the Milman-Chu vectors perform almost identically as the eigen mode sensitivity vectors in accelerating the convergence of the Galerkin procedure. A major advantage of the Milman-Chu modes over the eigen mode sensitivities is that they can be calculated much more economically. Since the Milman-Chu (M-C) vectors perform as well as the eigen mode sensitivity vectors, they are used exclusively in the following.

In the calculations presented, the M-C vectors were made orthonormal with respect to the mass matrix to each of the eigen modes employed. This in no way changes the configura-

tion space available to the Galerkin algorithm, but it makes interpretation of the calculated generalized coordinates easier.

Chapter 3

Model Reduction for a Structure Containing a Mechanical Joint

The major source of nonlinearity in structural dynamics is the localized frictional slip processes at interfaces in mechanical joints. The two important qualitative properties of mechanical joints - softening and dissipation - are illustrated in Figures 17 and 18. With respect to the first figure, one sees that under small load, the force-displacement curve appears nearly linear, though there is some amount of micro-slip and dissipation taking place even there. At larger loads, the force-displacement curve begins to level off and at very high loads macro-slip takes place and the tangent stiffness goes to zero. The second figure shows the power-law relationship between the amplitude of oscillatory load and the dissipation per cycle that is commonly seen experimentally over large load ranges. Mechanical joints manifest very little rate dependence.

The usual process of dealing with the presence of joints in structural dynamics is to represent the joint compliances by tunable springs and to represent the joint dissipation by modal damping. The resulting tuned linear models are of course of little value except at the excitation amplitudes at which the structure is calibrated. A discussion of the limitation of such approaches can be found in [11].

A interesting feature of mechanical joints that increases their interest in the world of nonlinear model reduction beyond their practical importance is the intrinsic path dependence to their force-displacement properties. This feature is referred to as non-locality in the sense that the full state of the system cannot be known solely from the current values of kinematic variables and their rates. The nonlocality would appear to proscribe rigorous application of a number of otherwise powerful mathematical tools - including the use of nonlinear normal modes.

We shall introduce a particular constitutive model for joints so that we may explore the model reduction technique of this report in context of problems of practical importance.

Whole-Joint Approximation

Modeling the complexity of interface mechanics in the midst of structural dynamics calculations would be impractical. A tractable approach involves the introduction of a class of approximation that reduces the complexity of the contact problem to a small number of scalar constitutive equation. This approximation constrains the kinematics of all degrees of freedom on each side of the contact patch to a single kinematic variable. Corresponding kinematic variables on opposite sides of the interface are connected by a single scalar constitutive equation each. Such approximations are called "whole-joint" models. The whole-joint approximation currently employed in Sandia codes imposes multi-point constraints to cause surface nodes on each side of the interface to be constrained rigidly to a centralized node on that surface (Figure 19). In the absence of more complete knowledge of joint physics, the constitutive equations for the six relative degrees of freedom are treated as being independent.

The Four-Parameter Iwan Model

A constitutive equation consistent with the more important qualitative joint behavior observed experimentally is the four-parameter Iwan model discussed in [10] and [12]. This model is an instance of Iwan's parallel-series configuration ([3], [4]) represented graphically in Figure 20 showing a continuum of Jenkins elements. All the spring stiffnesses are identical, so the model response is determined entirely by the population density ρ of Jenkins elements of given slider strengths ϕ. The mathematics of such models is discussed in depth in the papers of the above four citations.

The 4-parameter Iwan model is defined as follows:

$$\rho(\phi) = R\phi^{\chi}\left[H(\phi) - H(\phi - \phi_{\max})\right] + S\delta(\phi - \phi_{\max}) \tag{3.1}$$

where $H()$ is the Heaviside step function and the the process for finding parameters R, S, χ, and $\phi_{\max}$ is found in [10] and [12] . Values of $-1 < \chi < 0$ results in power-law exponents of $3 + \chi$. The general form of this 4-parameter distribution is shown in Figure 21. A major deficiency of the above set of parameters is the fractional dimensions of R and S so an alternate and preferred set of parameters (F_S, K_T, χ, and β) for this model have been developed [12]. In the following we use values

$F_S = 1.0$	the force that initiates macro-slip.
$K_T = 1.0$	joint stiffness in the regime of small load.
$\chi = -0.5$	the dimensionless strength of the singularity at zero.
$\beta = 2$	a dimensionless parameter having to do with the shape of the dissipation curve.

Numerical Results for Problems of Micro-Slip

We first examine the results of a numerical experiment associated with the structure shown in Figure 3 but where the cubic nonlinearity is replaced with the Iwan model described above. In this case the amplitude of the triangular pulse is $F_0 = 0.5$ - just one half of the break-free force F_S of the joint. Referring to Figure 22, we see that a Galerkin solution using the first five eigen modes of the reference linear system does a very poor job of capturing the kinetic energy of this system, but a Galerkin solution using the first three elastic modes and a joint mode (Milman-Chu) performs very well.

We also see that once the excitation is complete, the energy of the system continuously declines because of the hysteretic nature of the joint. This joint damping plays a major role in mitigating the shock that weapons systems can experience in a hostile environment.

It is natural at this point to ask the question: if the joint mode is necessary to capture the mechanics of the system, how does it change the kinematics that would be observed from the transient solution. This question is addressed with reference to Figure 23 where we see that the generalized accelerations seem to be dominated by the first mode - as one would expect. One order of magnitude lower are the kinematics of the second mode and the kinematics of the third mode and the joint mode are an order of magnitude yet smaller. Each of the modes is mass normalized, so the contributions to the physical accelerations are roughly proportional to the generalized accelerations.

Recall also that in these simulations the Milman-Chu mode that is employed has been made orthogonal to the elastic modes with respect to the mass and stiffness matrices. The coupling evidenced by the peaks of the generalized acceleration associated with the M-C mode occurring at frequencies of the peaks of the generalized accelerations of the elastic modes is purely a nonlinear effect. Because the Milman-Chu mode has been made orthogonal to only the first three elastic modes, it carries some part of the shapes of higher modes and the peaks of the corresponding generalized accelerations at higher frequencies are reflective of modes at those frequencies.

In the following simulations we highlight both the softening and dissipative features of mechanical joints through simulations of base excitation experiments. Again, we consider an eleven mass system with the nonlinear element placed between the fifth and sixth masses. This configuration is illustrated in Figure 24.

In these experiments, we employ an impulse of a sort that is increasingly popular in base excitation experiments - the Morlet wavelet of frequency 4:

$$f(t) = A_0 \cos(\omega 2\pi t/\tau) \exp\left(\frac{(2\pi t/\tau)^2}{2}\right) \tag{3.2}$$

where A_0 is the peak amplitude to be obtained, τ is the period of the frequency to be excited, and ω defines the shape of the wavelet. In the experiments presented here $\omega = 4$ and the

characteristic shape is shown in Figure 25.

In the first set of numerical experiments the max impulse is set to $F_0 = 0.005$ and Figure 26 shows that the resulting joint force calculated from the full spatial solution stays well below the break-free force F_0 of the joint. The corresponding portion of the monotonic force-displacement curve for the joint is shown along with the tangent stiffness at zero load in Figure 27. One expects such excitations to cause very little nonlinear response in the joint.

Indeed Figure 28 shows that the Galerkin solution employing eigen modes of the reference linear system generates a very good approximation for the kinetic energy of the jointed system subject to a small amplitude impulse. There is so little nonlinearity at the joints that the linear eigen modes do a good job of spanning the configurations taken on by the jointed structure. The presence of the joint is indicated only by the decrease in system energy over time due to dissipation in the joint.

One could also anticipate the adequacy of the eigen modes of the RLS in solving this low amplitude problem by consideration of Figures 29 and 30 obtained from the full nonlinear spatial solution. The first shows that the nonlinear system response is limited to resonance of just the first natural frequency of the reference linear system and the second shows that the first SVD mode of the numerical solution is almost identical to the first eigen mode of the RLS.

Interestingly Figure 31 shows that even for the nearly linear case discussed in this section, the use of a single Milman-Chu joint mode greatly increases convergence of the reduced order model to the solution of the full system.

When the amplitude of the base excitation is raised to $A_0 = 0.02$, the elastic modes are a much less satisfactory basis of modeling the more nonlinear system. Figure 32 shows that three elastic modes augmented with a Milman-Chu mode provide a much better basis for modeling vibration ring-down in this problem than are six elastic modes. Though not shown here, the peak joint force encountered in this simulation is approximately 70% the break-free force F_S.

The generalized accelerations shown in Figure 33 show behavior similar to that presented in Figure 23. Again, we see that though the joint mode is necessary for capturing the correct mechanics in this problem, it mode does not make a strong appearance in the structural kinematics.

Numerical Results for Problems of Macro-Slip

A Galerkin solution using just the eigen modes of the reference linear system is dramatically less successful for problems where applied loads approach or exceed the break-free force F_0 of the joint.

In the cases considered here, the amplitude of input wavelet is 0.05 and the resulting joint load history predicted by the full nonlinear spatial solution is shown in Figure 34. We see here that the joint is brought into macro-slip and peak force levels in the joint are saturated at F_S until enough energy has dissipated that the system loads on the joint drop to lower levels. This force history on the joint corresponds to the monotonic force-displacement curve shown in Figure 35, where the strong nonlinearity is illustrated by its contrast to the zero-load tangent stiffness curve.

The nonlinearity that the joint lends to the system dynamics is suggested by the plots of the first SVD mode of the full nonlinear spatial solution and the first eigen mode of the reference linear system in Figure 36. Note that these curves are quite different in the vicinity of the joint.

Another indication of the strong nonlinearity of this system is shown in Figure 37. Here we see that the acceleration of the right hand mass of the system contains not only components at the frequency of the excitation (which was tuned to the first natural frequency of the reference linear system), but also many higher frequency components.

Given the above, it should be no surprise that Galerkin solution using just the eigen modes of the reference linear system demonstrates very poor performance. In Figure 38 we see that even with ten elastic modes, the kinetic energy is approximated very poorly despite the fact that those modes correspond to much higher frequencies in the linear system than are indicated in Figure 37. The transitions to macro-slip in this problem appear to be responsible for the transfer of energy from the low excitation frequency to much higher frequencies. As expected, when sufficient modes to reach the frequency response of the corresponding linear system are augmented by a joint mode, the system is modeled much better (Figure 39). Figure 40 shows that the augmented basis set captures the correct character of the magnitude of the Fourier transform of acceleration of the right-most mass, while the approximate solution that employs only the elastic eigen modes leaves too much energy at the lower frequencies.

That the displacement across the joint in macro slip can be an appreciable part of the overall kinematics is evidenced in Figure 41 where the generalized acceleration associated with the joint mode is comparable with that of the first linear vibration mode.

An interesting result is found when a "ruthlessly reduced" model is employed. When this large amplitude experiment, resulting in high frequency components in the structural response, is approximated by three elastic eigen modes and one joint mode, the kinetic energy predicted (Figure 42) is in noticeable error. However, the error is substantially less than that of the Galerkin solution where eight elastic eigen modes but no joint mode are employed.

Particularly intriguing is the predicted acceleration of the right-most mass. In Figure 43 the accelerations predicted by the very reduced model appear as though they were the full spatial solution as seen through a low-pass filter. That hypothesis is tested by comparing the full solution and the very reduced solution when both are sent through a low-pass filter.

(Sixth order Butterworth filter with cut-off frequency 0.03). The results shown in Figure 44 do argue that for the special case of these Iwan joint models, a low-order model for the full non-linear structure seems to capture the low frequency response of the structure reasonably well. Why this reduced order model works so well for these joint models is not entirely clear at this time, though one would have every reason to believe that such fortuitous results would not occur for a rate-type nonlinearity.

Chapter 4

Implementation in the Context of Finite Element Analysis

The tools presented in this report are intended to facilitate predictive structural dynamic simulation, and that means integration into finite element analysis. Most of the necessary components for large scale analyzes of jointed structures are available in standard finite element packages, including eigen analysis and elastic static analysis. Additionally, the techniques presented here seem to be complementary to other model reduction methods - component mode synthesis especially.

Automatic Determination of Special Vectors and Matrices

The only quantities whose construction is not obvious are the vector F_j aligned along the joint j, the tangent stiffness matrix $K_N(\{s_j\})$, and the Milman-Chu vectors $y_{MC,j}$.

Algebraic Vector F_j

In the simplest case, when the joint is aligned in a principle direction, the vectors F_j are constructed by putting a 1 in the entry associated with the degree of freedom of the first joint node and the joint direction and a -1 in the entry associated with the degree of freedom of the second joint node and that joint direction.

On the other hand, the task is more difficult when the joint is aligned in a local coordinate system and here we discuss a formal strategy for deducing F_j in such general circumstances. Recall that K_0 is the stiffness of the reference linear system, where each joint j is represented by a properly oriented spring of stiffness k_j. Let's define K_j to be the corresponding stiffness matrix when the equivalent spring for joint j is replaced by a spring of stiffness

$k_j + \delta k_j$. The difference matrix $\delta K_j = K_j - K_0$ will have nonzero entries only for degrees of freedom associated with the nodes associated with that joint. For an extensional joint (or a torsional joint), those entries map to a six by six matrix $K_{6,j}$ which has only one nonzero eigen value. Let $\hat{F}_j$ be the corresponding eigen vector, normalized so that $\hat{F}_j^T \hat{F}_j = 2$ and let F_j be that vector mapped back to the full system.

Gradient Matrix K_N

In solving the nonlinear dynamic equations numerically one often employs methods such as Newton iteration which require taking the gradient of all terms in the governing equation with respect to all the kinematic variables. The relevant gradient of the joint terms are neatly merged to those of the stiffness matrix of the reference linear system in the following manner

$$K_N = K_0 + \sum_{\text{joints } j} G_j \left(\frac{d f_j(s)}{ds} - k_j \right) \tag{4.1}$$

where

$$G_j = F_j F_j^T \tag{4.2}$$

Milman-Chu Algebraic Vector $y_{MC,j}$

The Milman-Chu vector associated with joint j is easily constructed by performing a static analysis associated with applying equal and opposite loads on the joint nodes in the direction of the joint alignment while applying no loads at other joints or external boundaries.

Employment in Conjunction with Component Mode Synthesis

The model reduction method presented here addresses difficulties particularly associated with local nonlinearities. It is consistent with other model reduction methods - the method of component mode synthesis in particular.

Consider a structure $\mathcal{B}$ consisting of a number of substructures $\mathcal{B}_k$ with joint models connecting some of the interface degrees of freedom. The kinematics of each substructure is characterized by the values of interface degrees of freedom $\{u_{k,n}\}$ and modal degrees of freedom $\{\phi_{k,n}\}$. The development of the reduced order model proceeds much as discussed earlier in this report:

- eigen analysis is performed on the linearized component mode representation for $\mathcal{B}$.
- the Milman-Chu vector is calculated by placing self equilibrating loads on nodes on the interface between substructures and performing a system level statics solution.
- the numerical results are in terms of vectors whose support is the whole structure.

How Many Modes?

The number of elastic modes and Milman-Chu modes necessary for application to a particular problem can be estimated in a manner similar to that employed in modal truncation of linear systems. In the simplest implementation, one employs all elastic modes corresponding to frequencies below an appropriately chosen cut-off frequency and one uses a Milman-Chu mode for each joint degree of freedom.

Chapter 5

Conclusion

We have demonstrated the feasibility of achieving reduced models for systems with localized nonlinearities by augmenting the most natural basis functions with vectors that have appropriate discontinuities at the locations of nonlinearity. This assures that the kinematics necessary to couple the nonlinearity to the rest of the structural response are present.

Though this model reduction appears to work well for both large and small structural loads, a few words are appropriate about how the results manifest themselves for the cases of small loads. It is observed in the examples shown here that for such cases the amplitude of the generalized coefficient for the discontinuous basis function is always very low compared to those of the first several elastic eigen modes. The augmenting mode serves the purpose of coupling the joint mechanics into the dynamics of the other modes. In doing so it does not change the characteristic mode shapes as seen by SVD, it just provides modest nonlinear damping. In these ways, the apparent modal response of the reduced nonlinear systems appears very much like that found in a modal lab for real structures: one sees apparently linear modes, except for nonlinear damping of each mode.

It is natural for practitioners of several areas of applied analysis to identify the technique presented here with some of the basis functions common in their areas and some of those identifications are correct. For instance one might identify the joint modes presented here with the constraint modes or attachment modes ([2]) of component mode synthesis. Those comparisons are incomplete. Constraint modes and attachment modes live solely on individual sub-structures while the support for the joint modes presented here live over the entire structure. (It should be pointed out that one could create functions with the necessary discontinuity through combinations of constraint modes, but the suitability of such functions as joint functions has not yet been explored.) Perhaps better analogues to joint modes are hydrodynamic doublet fields or the displacements in a crystal lattice due to the presence of a point dislocation.

The most important observation - regardless of what analogies one wishes to make - is that it is because of the mechanical coupling of those joint modes with the eigen modes

of the reference linear structure that those eigen modes satisfactory describe the nonlinear structural dynamics.

The utility of the approach presented here will be explored in future work applying these tools to increasingly large finite element problems. Ultimately, we hope to demonstrate the natural complementarity between this technique and component mode synthesis by converting problems of millions of degrees of freedom to ones of thousands and then hundreds.

Appendix: Nonlinear Normal Modes

Because Nonlinear Normal Modes (NNMs) have proven helpful in understanding the dynamics of many nonlinear systems, it is helpful to discuss the approach presented here in terms of NNMs in the hope of expanding the utility of NNMs in structural dynamics.

In the sense of Pesheck et al. [9] the existence of a nonlinear normal mode is equivalent to the assertion that the deformation field at any time can be expressed

$$u(t) = A(t)\,y_1 + \sum_{n=2}^{N} P_n(A,\dot{A})\,y_n \tag{A-1}$$

where vectors $\{y_n\}$ are a displacement basis for the structure, A is a periodic function of time, and the coefficient functions P_n are characteristic of the system. Usually, all basis vectors are chosen to be the eigen modes of the reference linear system.

The similarity of equations 2.3 and A-1 and the numerical calculations of the previous section permit us to make the following assertion: *For structures containing localized nonlinearities, unless the set of basis functions is selected to include some with the appropriate discontinuities, expansions such as the above cannot converge to the true solution.*

On the other hand, the analysis technique explored in the previous chapter does employ basis vectors with the appropriate discontinuity so it might be profitable to see if that technique yields solutions containing any of the character of nonlinear normal modes. We consider "ruthlessly-reduced" cases using as basis vectors just the first eigen mode of the reference linear system and a Milman-Chu vector. We perform simulations for $F_0 = 0.05$, $F_0 = 0.1$, and $F_0 = 0.5$.

The nonlinear normal mode expression corresponding to our two-basis element Galerkin formulation is

$$h(t) = A(t)y + f(A(t))w \tag{A-2}$$

In the context of Equation 2.3, $a_1 = A(t)$ and the assertion of this being a nonlinear normal

mode would be

$$a_2(t) = f(A, \dot{A}) \tag{A-3}$$

We examine the results of our transient numerical calculation to assess if Eq. A-3 is satisfied. Figure A-1 shows plots of $a_2(t)$ vs $a_1(t)$ for each of our three cases. These plots are obscured by gray clouds of higher frequency components. When the phase space $(a_1, \dot{a}_1)$ is distributed into bins (a_1 x $\dot{a}_1$ into 15x5 bins) and the values of a_2 in each bin in averaged, the points shown in dark squares results. The lack of scatter in these dots indicates the absence of velocity dependence - as one would expect for a perfectly elastic system.

The averaged results of the previous figure are plotted together in Figure A-2 and indeed the data are consistent with an assertion that a_2 is some function of a_1. This is the the assertion of the manifestation of a nonlinear normal mode.

Let's now see how consistent these results are with a simple nonlinear normal mode calculation. Recall that the joint mode (Milman-Chu in this case) is made orthonormal with respect to the mass matrix to the linear eigen modes that employed. Say that $y = y_1$ is the first eigen mode of the RLS and w is the M-C mode made orthonormal to y with respect to the mass matrix:

$$y^T M y = 1 \quad y^T M w = 0 \quad w^T M w = 1 \tag{A-4}$$

Contraction of these vectors with the stiffness matrix yields the Rayleigh quotients

$$y^T K y = \omega_0^2 \quad w^T K w = \hat{\omega}^2 \tag{A-5}$$

where ω_0 is the natural frequency of the first eigen mode of the RLS and $\hat{\omega}$ is a number greater than or equal to the second natural frequency of the RLS. (This is the minimax principle. [7])

We do not know much about the evolution of this NNM, but we can assert that the system is conservative so that the kinetic energy when the system velocities are maximum equals the strain energy when the system displacements are greatest. The maximum kinetic energy is

$$\begin{aligned} \mathrm{KE}_{\max} &= \tfrac{1}{2}\dot{A}_{\mathrm{m}}^2 \left(y + f'(A)w\right)^T M \left(y + f'(A)w\right) && \text{(A-6)} \\ &\approx \tfrac{1}{2}\omega_0^2 A_{\mathrm{m}}^2 \left(1 + f'(A)^2\right) && \text{(A-7)} \end{aligned}$$

where A_{m} is the maximum value taken on by $A(t)$ during the cycle, $\dot{A}_{\mathrm{m}}$ is the maximum value taken on by $\dot{A}(t)$ during the cycle, $f'(A) = df(A)/dA$, and we have assumed that $\dot{A}_{\mathrm{m}} = \omega_0 A_{\mathrm{m}}$.

The maximum strain energy is

$$\mathrm{SE}_{\max} = \frac{1}{2}\left(A_{\mathrm{m}} y + f(A_{\mathrm{m}}) w\right)^T K \left(A_{\mathrm{m}} y + f(A_{\mathrm{m}}) w\right)$$

$$+ N\left(A_{\mathrm{m}}\,\delta y^* + f(A_{\mathrm{m}})\delta w^*\right) \tag{A-8}$$

where N is the nonlinear part of the strain energy at the joint. In the case of our cubic spring,

$$N(\delta u) = K_2 \delta u^4/4 \tag{A-9}$$

The maximum strain energy is now

$$\mathrm{SE}_{\max} = \frac{1}{2}\omega_0^2 A_{\mathrm{m}}^2 + \frac{1}{2}\hat{\omega}^2 f(A_{\mathrm{m}})^2 + N\left(A_{\mathrm{m}}\,\delta y^* + f(A_{\mathrm{m}})\delta w^*\right) \tag{A-10}$$

where δy^* and δw^* are the displacements across the nonlinear joint of y and w respectively and N is the strain energy associated with the essential nonlinearity. When we equate the two energies (Equations A-7 and A-10, we obtain an equation for f'

$$\omega_0^2 A_{\mathrm{m}}^2\, f'(A)^2\, w = \hat{\omega}^2 f(A_{\mathrm{m}})^2 + 2N\left(A_{\mathrm{m}}\,\delta y^* + f(A_{\mathrm{m}})\delta w^*\right) \tag{A-11}$$

which can be solved numerically for $f(A)$. These results are shown in Figure A-3 along with the data shown previously in Figure A-2. We see a strong similarity between the NNM prediction and the values deduced from post-processing of simulations and we also see systematic differences that can be attributed to the ambitious effort to represent the system dynamics with just two basis vectors.

References

[1] C. Chu and M. H. Milman. Eigenvalue error analysis of viscously damped structures using a ritz reduction method. *AIAA Journal*, 30:2935–2944, December 1992.

[2] R.R. Craig. *Structural Dynamics: An Introduction to Computer Methods*. Wiley, 1981.

[3] W. D. Iwan. Distributed-element model for hysteresis and its steady-state dynamic response. *ASME Journal of Applied Mechanics*, 33(4):893–900, Dec. 1966.

[4] W. D. Iwan. On a class of models for yielding behavior of continuous and composite systems. *ASME Journal of Applied Mechanics*, 34(3):612–617, 1967.

[5] L. V. Kantorovich and V. I. Krylov. *Approximate Methods of Higher Analysis*. Interscience, New York, 1958. (translated from Russian).

[6] G. Kerschen, J. C. Golinval, A. F. Vakakis, and L. A. Bergman. The method of proper orthogonal decomposition for dynamical characterization and order reduction of mechanical systems: An overview. *Nonlinear Dynamics*, 41(1-3):147 – 169, August 2005.

[7] S. G. Mikhlin. *Mathematical Physics: an Advanced Course*. American Elsevier Publishing Company, Inc., New York, 1970.

[8] M. H. Milman and C. C. Chu. Optimization methods for passive damper placement and tuning. *Journal of Guidance, Control, and Dynamics*, 17(4):848 – 56, Jul-Aug 1994.

[9] E. Pesheck, C. Pierre, and S. W. Shaw. New galerkin-based approach for accurate nonlinear normal modes through invariant manifolds. *Journal of Sound and Vibration*, 249(5):971 – 993, Jan 2002.

[10] Daniel J. Segalman. A four-parameter Iwan model for lap-type joints. Technical Report SAND2002-3828, Sandia National Laboratories, 2002.

[11] Daniel J. Segalman. Modelling joint friction in structural dynamics. *Structural Control and Health Monitoring*, 13(1):430–453, 2005.

[12] Daniel Joseph Segalman. A four-parameter iwan model for lap-type joints. *ASME Journal of Applied Mechanics*, 72(5):752–760, September 2005.

Figures

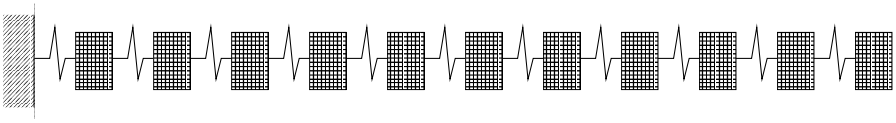

Figure 1. For purposes of illustration, we consider this simple system of eleven unit masses connected in a series manner to ground by a system of unit springs.

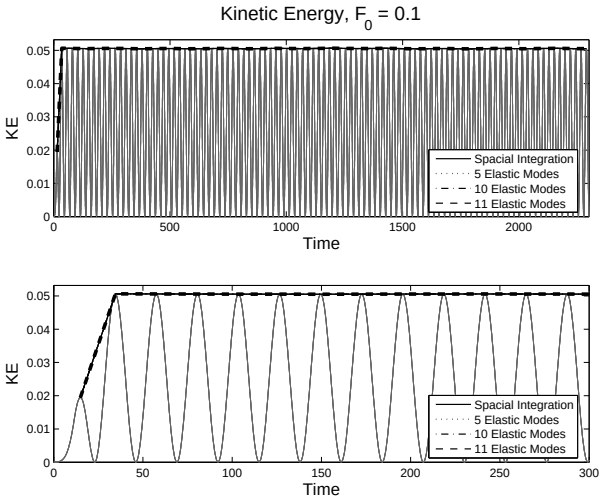

Figure 2. The response of the system shown in Figure 1 to a triangular pulse with peak force F_0 is calculated by the numerical solution for full spatial system (eleven degrees of freedom) and by several levels of modal truncation. In this and in similar plots, the legend refers to envelopes of the kinetic energy curves.

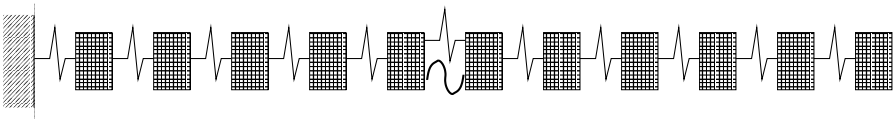

Figure 3. We consider this simple eleven unit masses connected in a series manner to ground by a system of unit spring. Additionally we place a cubic spring between the 5^{th} and 6^{th} masses of the system.

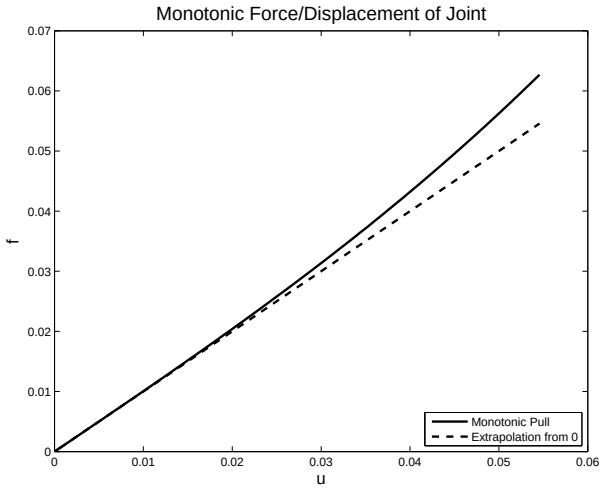

Figure 4. The response of a system with a small cubic nonlinearity appears almost linear so long as the excitations are also small. This figure is relevant to the following simulations where the peak force applied to the right hand side of the system is $F_0 = 0.05$.

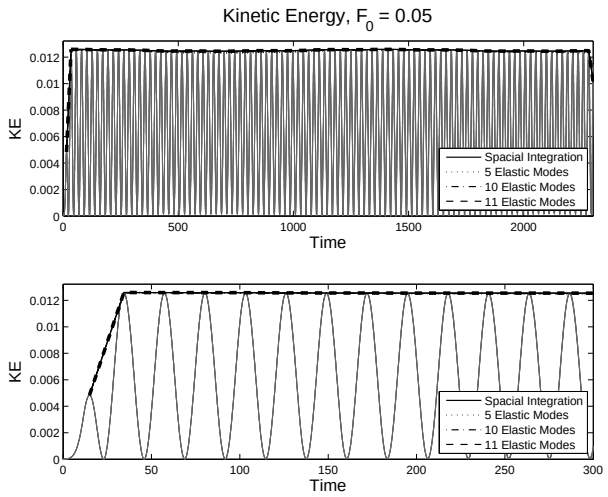

Figure 5. The kinetic energy of the system with a small cubic nonlinearity resulting from a triangularly shaped impulse. The Galerkin solution employing various numbers of eigen modes of the reference linear system provides a reasonably good approximation to this slightly nonlinear system.

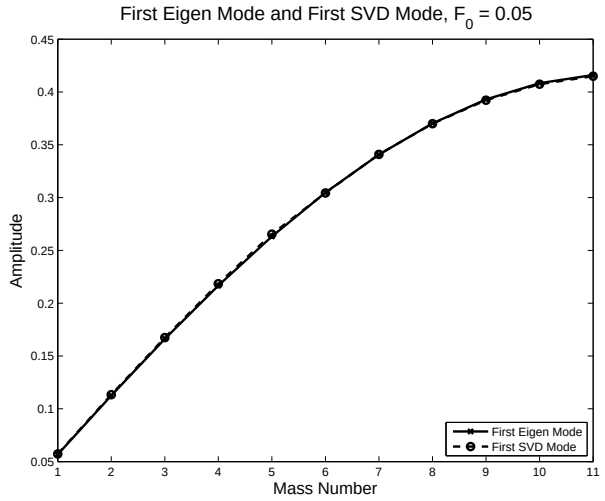

Figure 6. The response of a system with a small cubic nonlinearity is explored using the the singular value decomposition (SVD) modes of the history of the full nonlinear system. Shown here are the first SVD mode of the fully history and the first eigen mode of the RLS. For this small nonlinearity, both modes are almost identical.

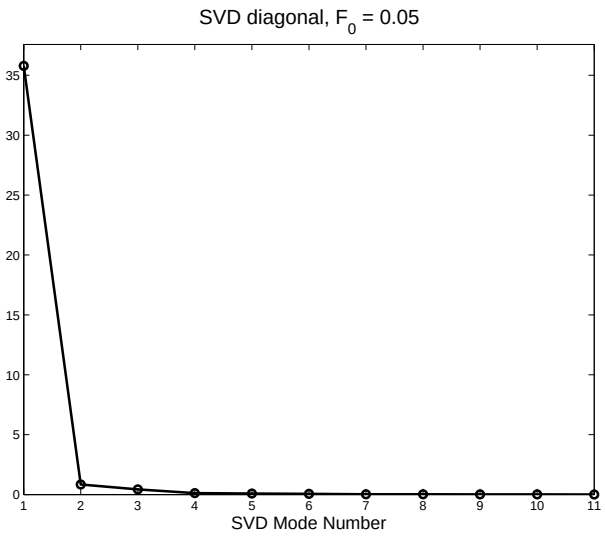

Figure 7. The response of a system with a small cubic nonlinearity is explored using the singular value decomposition (SVD) modes of the history of the full nonlinear system. The relative role of each SVD mode in the history is shown here. Only the first such mode is significant.

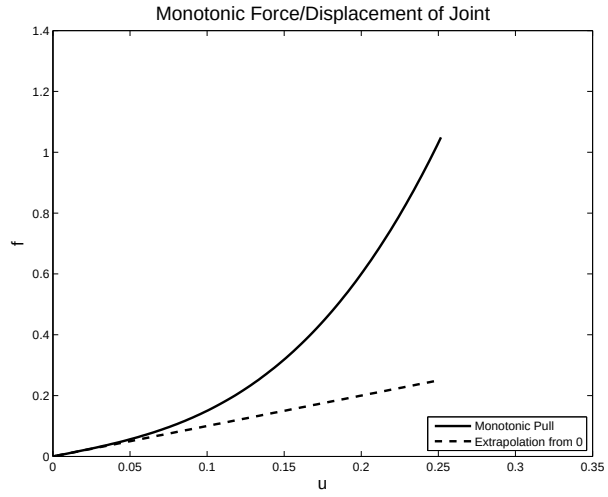

Figure 8. The response of a system with a cubic nonlinearity appears extremely nonlinear when the excitations are large. This figure is relevant to the following simulations where the peak force applied to the right hand side of the system is $F_0 = 0.5$.

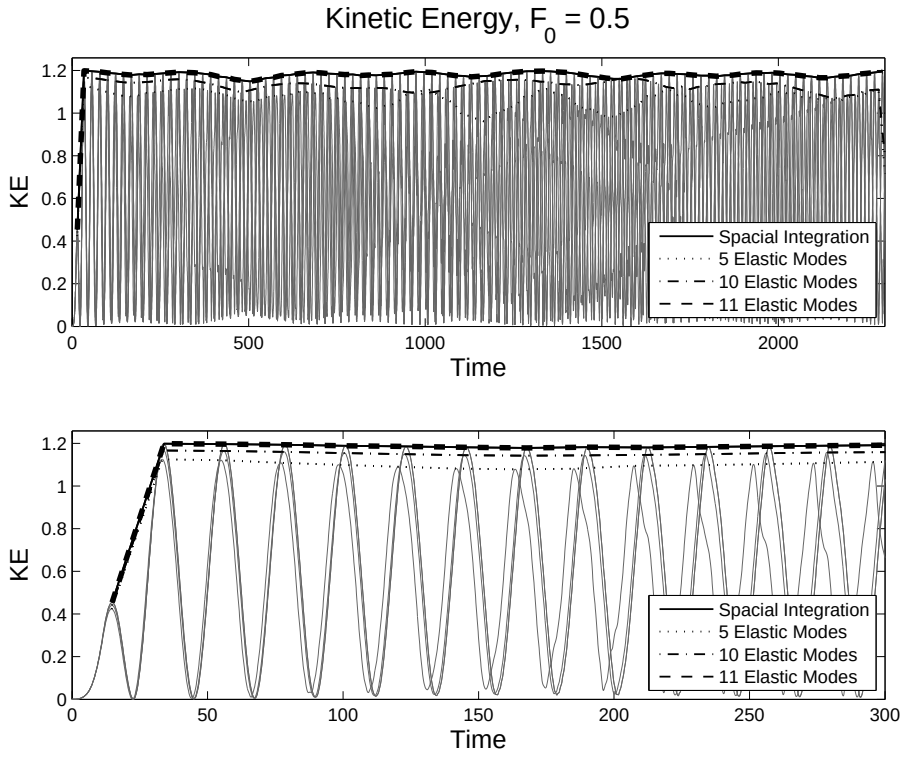

Figure 9. The kinetic energy of the system with a large cubic nonlinearity resulting from a large-amplitude, triangularly shaped impulse. The Galerkin solution employing various numbers of eigen modes of the reference linear system does not provide a good approximation to this nonlinear system unless the number of modes equals the total number of degrees of freedom of the physical system.

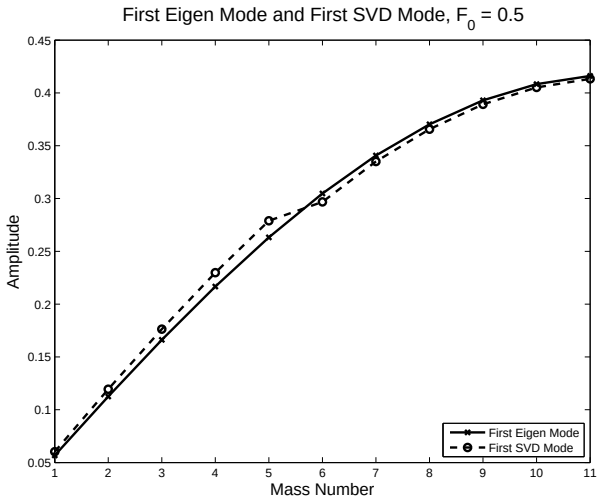

Figure 10. The response of a system with a large cubic nonlinearity is explored using the singular value decomposition (SVD) modes of the history of the full nonlinear system. Shown here are the first SVD mode of the full history and the first eigen mode of the RLS. For this large nonlinearity, the modes show a marked difference at the location of the nonlinear spring. Because there is a stiffening spring between the 5^{th} and 6^{th} masses, the SVD mode shows less deformation at that location than is the case of the linear eigen mode.

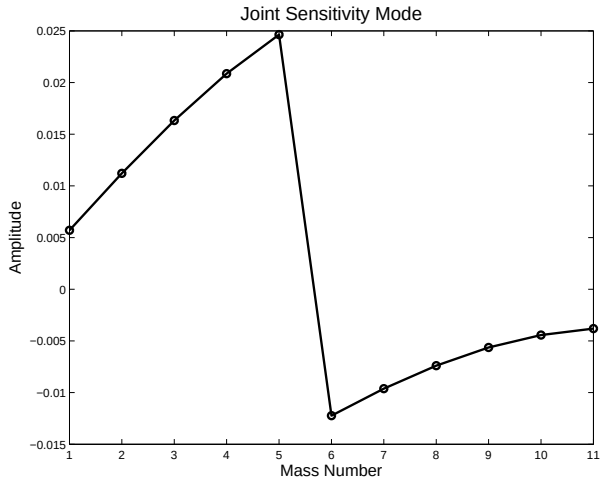

Figure 11. The sensitivity of the first eigen mode of the reference linear system with respect to stiffness at the location of the nonlinear spring manifests a discontinuity at that location.

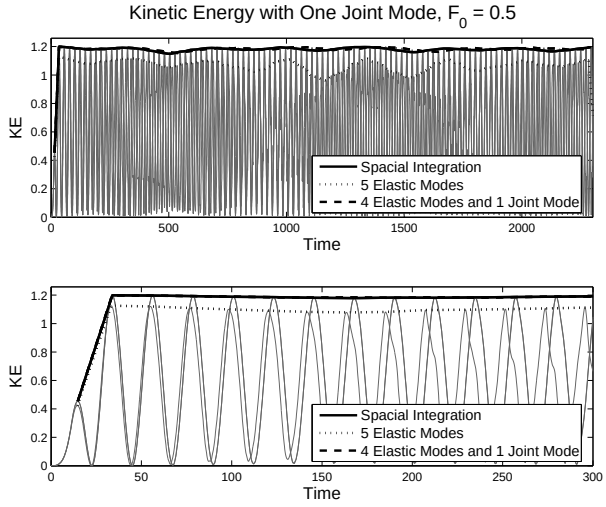

Figure 12. Convergence of the Galerkin procedure is greatly enhance when the basis includes an eigen mode sensitivity vector. In this case there are 4 eigen modes of the reference linear system and one eigen mode sensitivity vector.

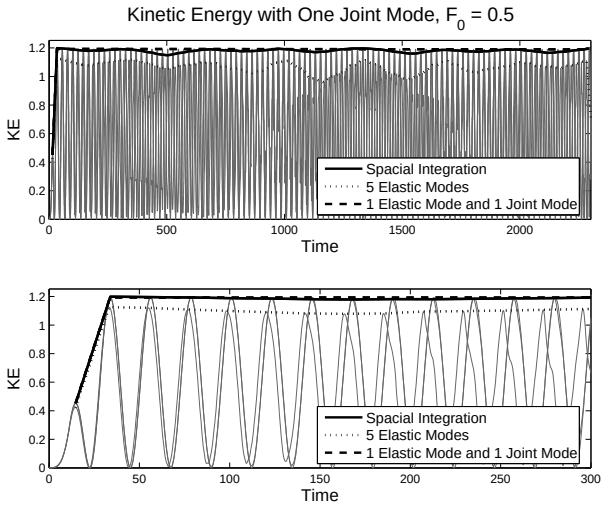

Figure 13. Convergence of the Galerkin procedure is greatly enhance when the basis includes an eigen mode sensitivity vector. In this case there are 1 eigen mode of the reference linear system and one eigen mode sensitivity vector.

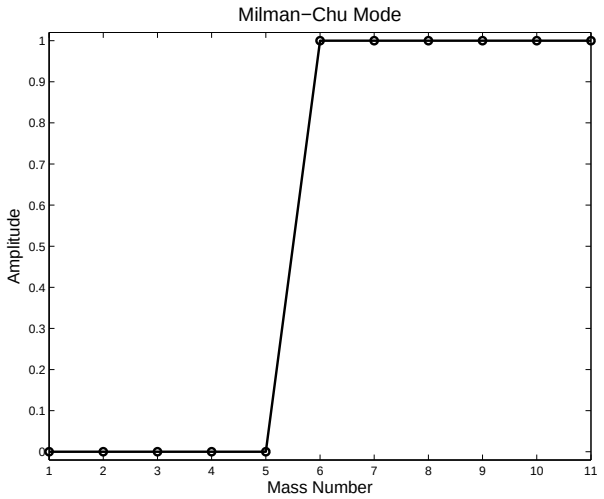

Figure 14. The Milman-Chu mode is the solution to a statics problem. It also has the discontinuity that is desired at the location of the local nonlinearity, but it is computed much economically than is the eigen mode sensitivity.

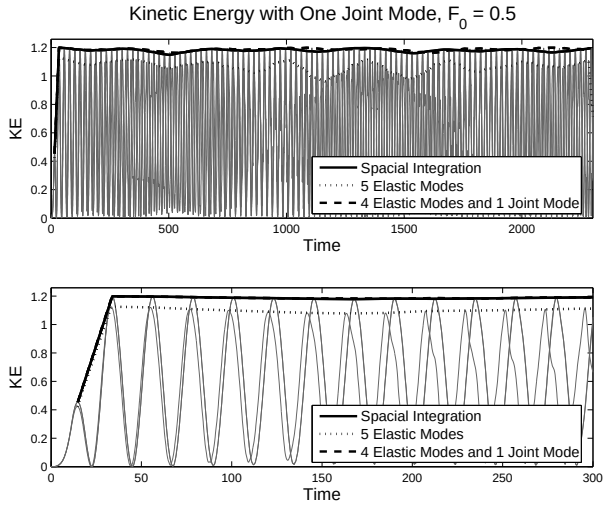

Figure 15. Convergence of the Galerkin procedure is greatly enhanced when the basis includes an Milman-Chu vector. In this case there are 4 eigen modes of the reference linear system and one Milman-Chu vector.

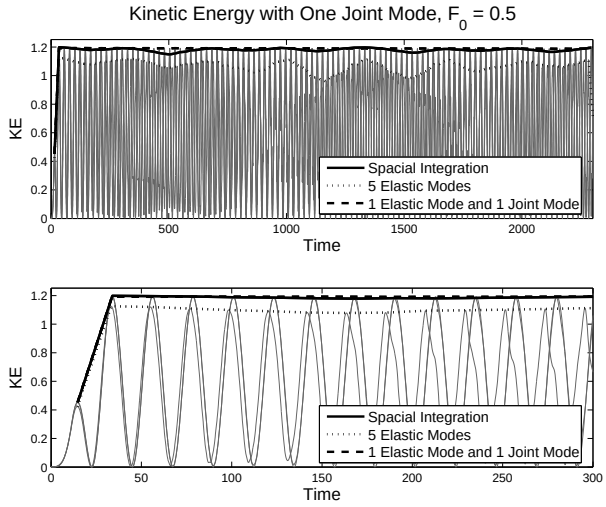

Figure 16. Convergence of the Galerkin procedure is greatly enhanced when the basis includes an Milman-Chu vector. In this case there are 1 eigen mode of the reference linear system and one Milman-Chu vector.

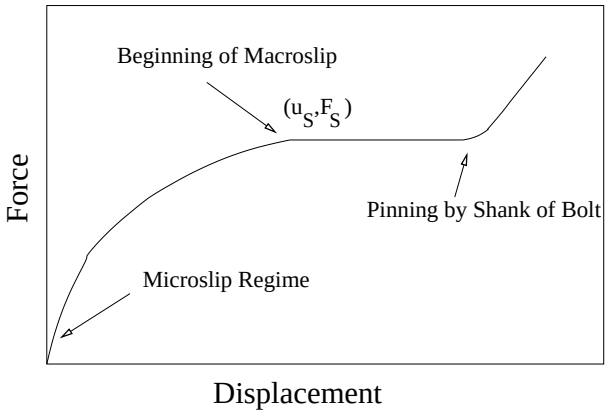

Figure 17. Mechanical joints manifest small regions of micro-slip where force-displacement appears linear, though some amount of dissipation accompanies any load. As the load increases, the tangent stiffness decreases until macro-slip initiates.

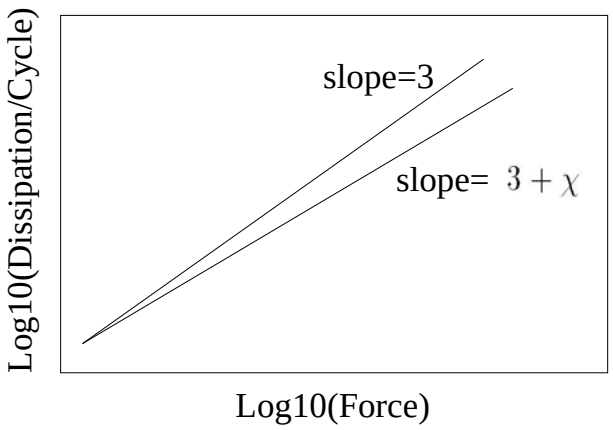

Figure 18. When mechanical joints are subject to oscillatory loads, the energy dissipation per cycle appears to increase with load amplitude in a power-law manner. In the above, χ is a number such that $-1 < \chi \leq 0$.

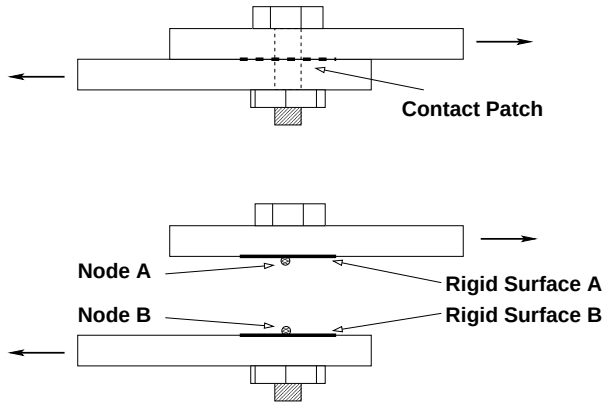

Figure 19. The mathematical complexity of the joint is simplified by approximating the whole interface by a single scalar constitutive equation for each of the six relative degrees of freedom. In the illustration shown here all of the nodes on each side of the interface are held rigid and connected to a single joint.

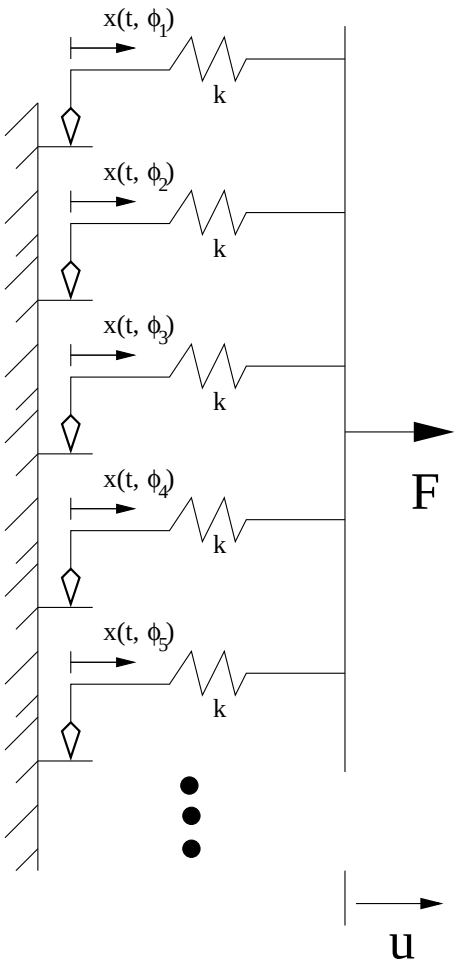

Figure 20. The parallel series Iwan model consists of a continuum of Jenkins elements. All the spring stiffnesses are identical, so the model response is determined entirely by the population density of Jenkins elements of given slider strengths.

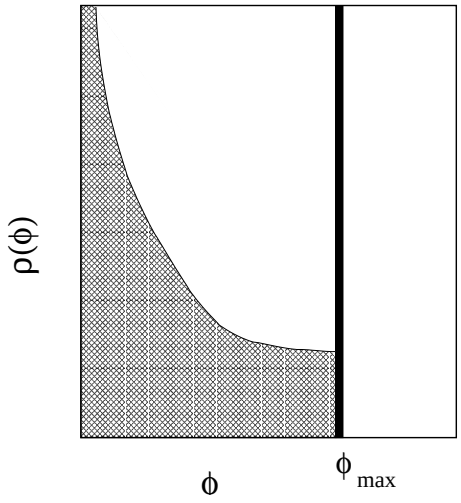

Figure 21. The four-parameter Iwan model predicts the correct qualitative behavior of mechanical joints.

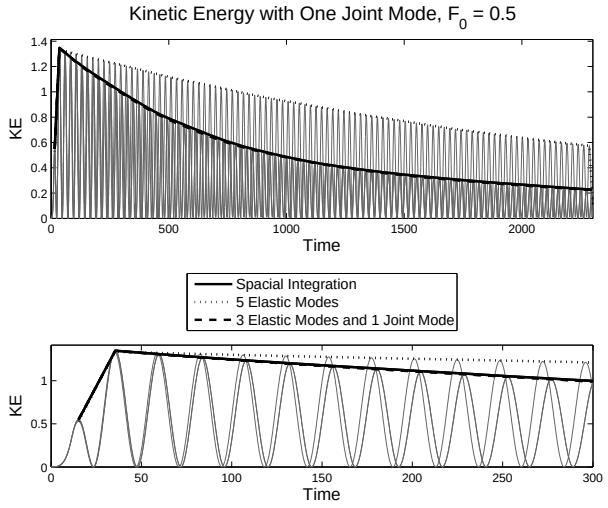

Figure 22. Convergence of the Galerkin procedure is greatly enhanced by the presence of Milman-Chu vector in this problem involving the structure shown in Figure 3, $F_0 = 0.5$, and a nonlinear Iwan joint model. In this case there are 3 eigen modes of the reference linear system and one Milman-Chu vector.

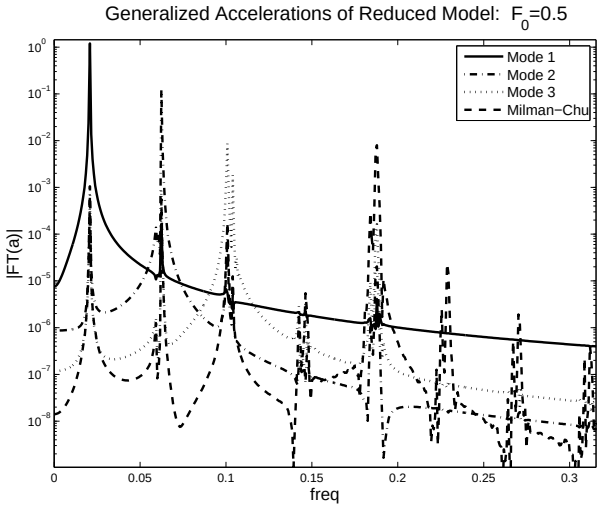

Figure 23. Though the presence of the joint mode among the basis vectors of the Galerkin calculation greatly accelerates convergence, the amplitude of the generalized acceleration associated with that vector is actually fairly small in this problem. Shown here is the magnitude of the Fourier transform (MFT) of acclera-tion.

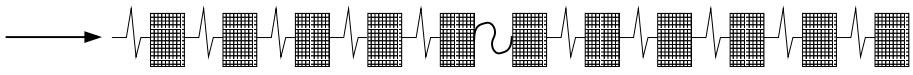

Figure 24. An eleven-mass system with a nonlinear joint excited at its base.

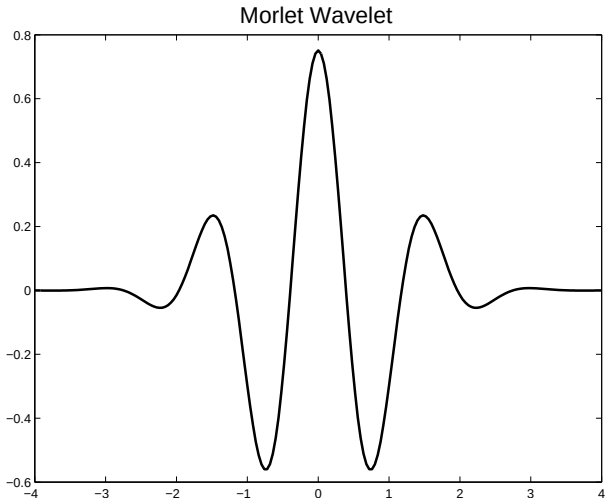

Figure 25. The Morlet wavelet with $\omega = 4$.

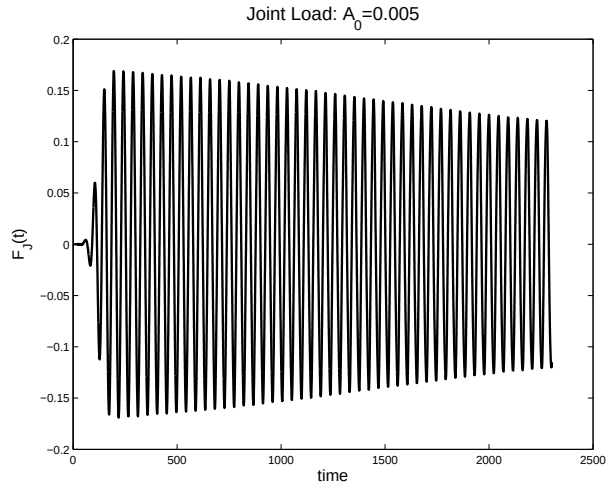

Figure 26. The force history of the joint resulting from a very low amplitude ($A_0 = 0.005$) base excitation.

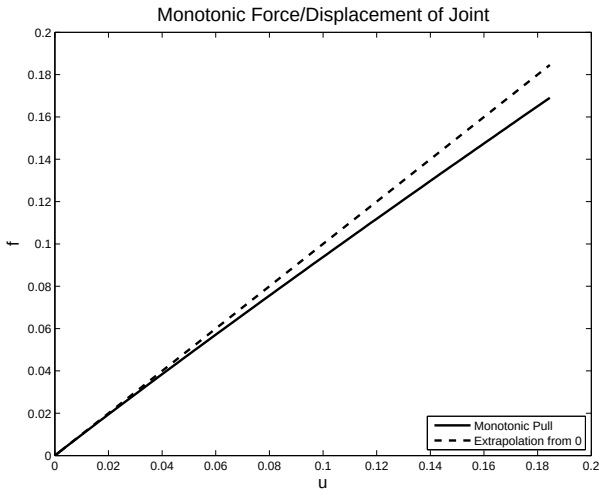

Figure 27. The force history of the joint resulting from a very low amplitude ($A_0 = 0.005$) base excitation corresponds to the above portion of the motonic force-displacement curve for the joint. Also shown is the tangent stiffness at zero load.

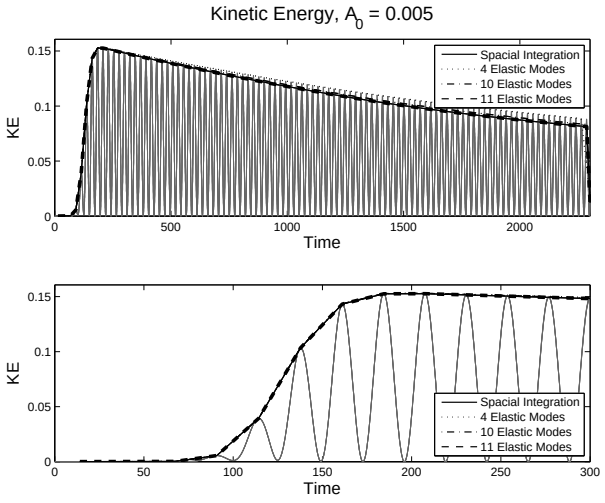

Figure 28. The Galerkin solution employing eigenmodes of the reference linear system generates a very good approximation for the kinetic energy of the jointed system subject to a small amplitude impulse ($A_0 = 0.005$).

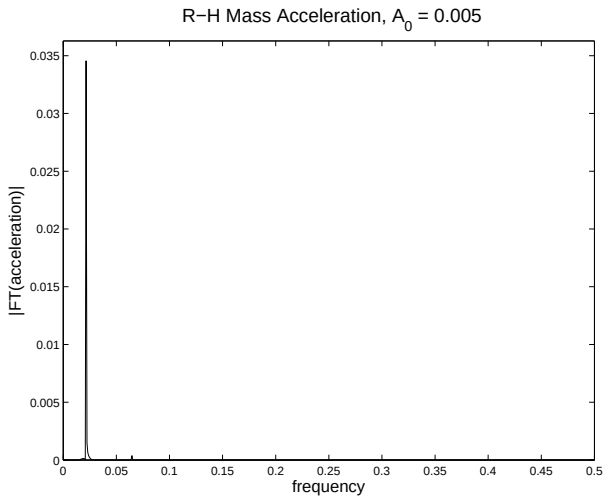

Figure 29. When subject to very small amplitude excitation ($A_0 = 0.005$), the system responds with a nearly monochormatic response at the frequency of excitation - which was tuned to the first natural frequency of the reference linear system.

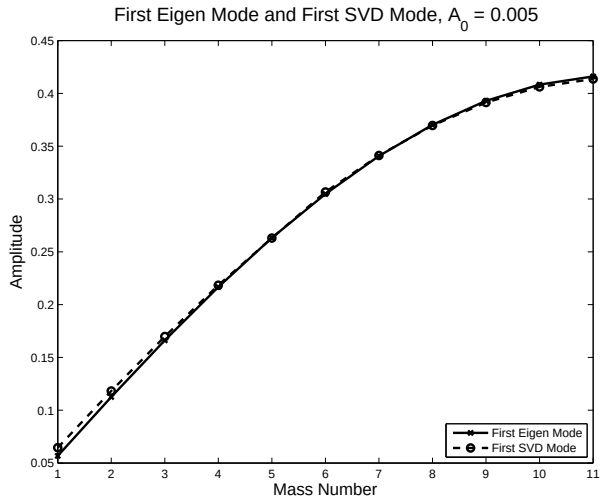

Figure 30. The SVD of the full nonlinear spatial solution and the first eigenmode of the reference linear system are nearly identical when the system is subject to a very low amplitude ($A_0 = 0.005$) base excitation.

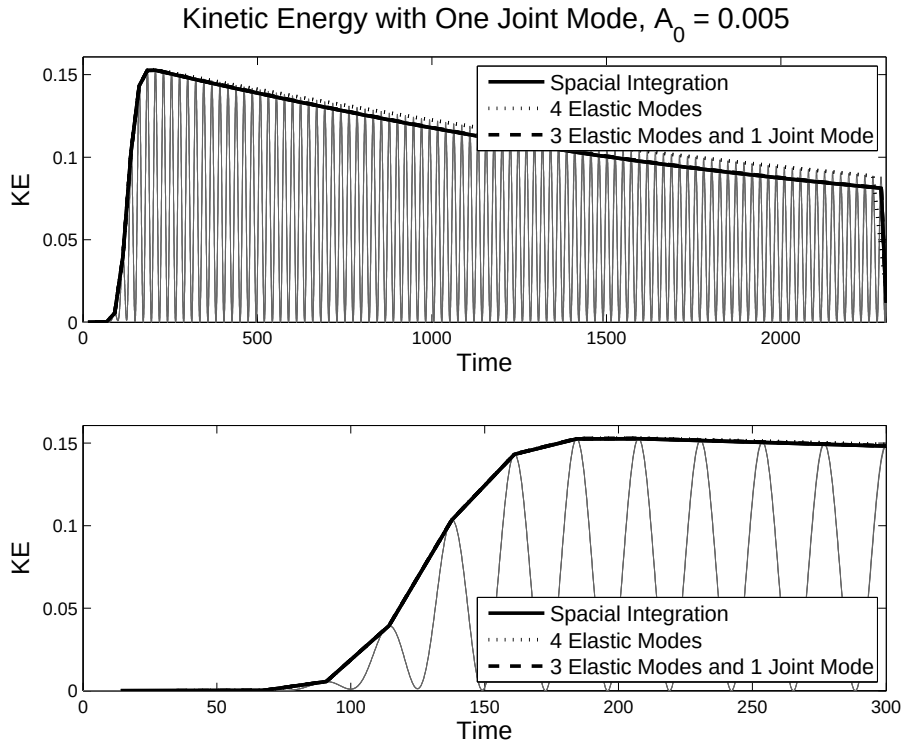

Figure 31. Even when the system is subject to a very low amplitude ($A_0 = 0.005$) base excitation, the use of a Milman-Chu joint mode makes a noticible improvement in convergence.

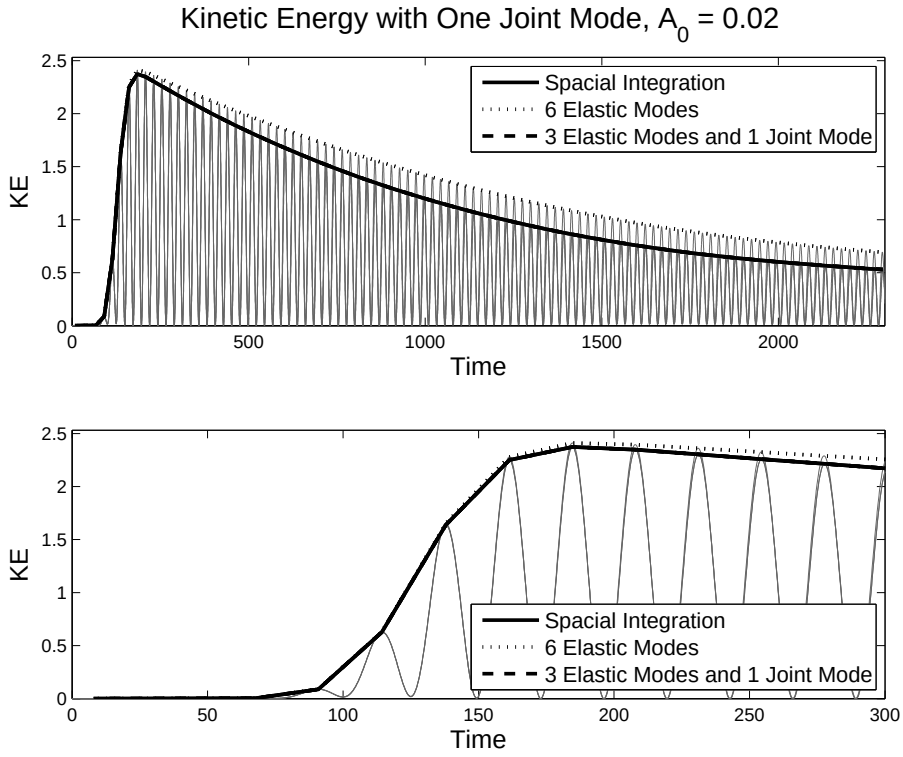

Figure 32. At a higher level of base excitation ($A_0 = 0.02$), the use of a Milman-Chu joint mode makes a more noticible improvement in convergence.

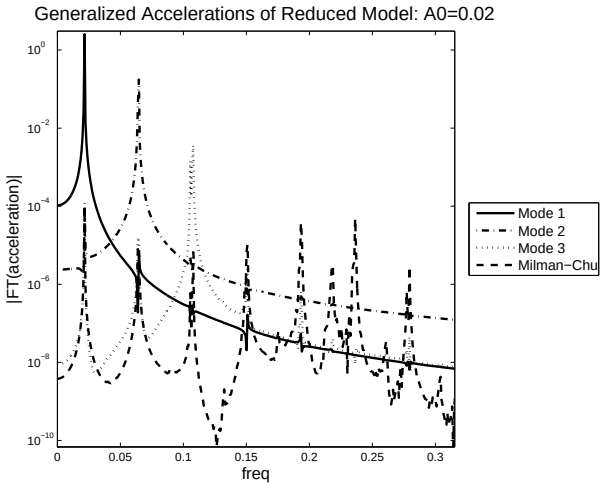

Figure 33. As was the case in the resonance calcuation of Figure 23, though the presence of the joint mode among the basis vectors of the Galerkin calculation greatly accelerates convergence, the amplitude of the generalized acceleration associated with that vector is actually fairly small in this base excitation problem ($A_0 = 0.02$).

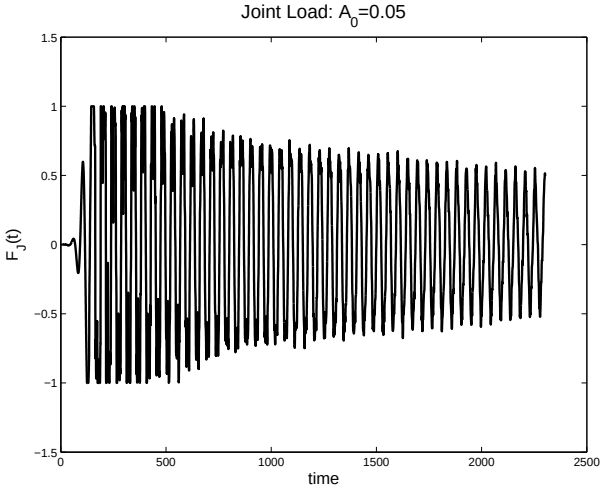

Figure 34. When the system is subject to a high amplitude ($A_0 = 0.05$) base excitation, the joint is brought into macro-slip and force levels in the joint are saturated at $F_J = F_S\ (= 1)$.

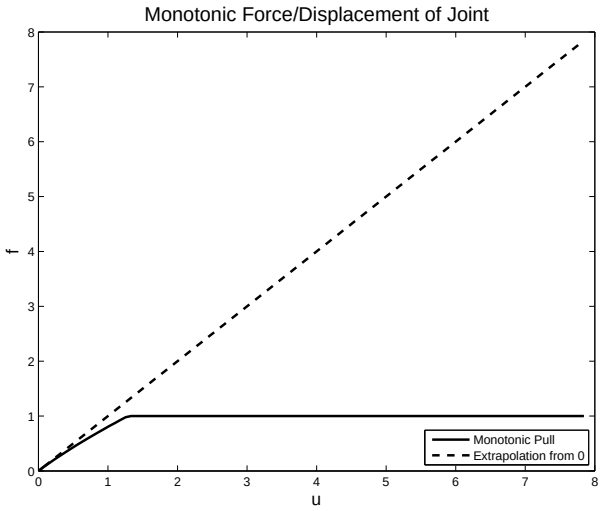

Figure 35. The force history of the joint resulting from a high amplitude ($A_0 = 0.05$) base excitation corresponds to the above portion of the motonic force-displacement curve for the joint. Also shown is the tangent stiffness at zero load. The nonlinearity manifest at these force levels is large.

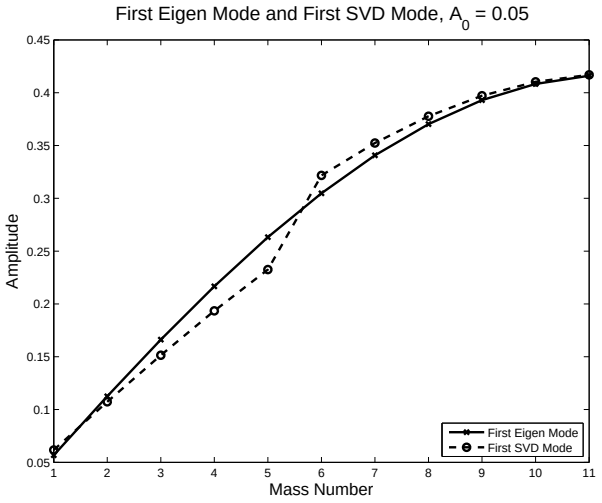

Figure 36. The first SVD mode of the full nonlinear spatial solution and the first eigenmode of the reference linear system are quite different in the vicinity of the joint when the system is subject to a high amplitude ($A_0 = 0.05$ base excitation.

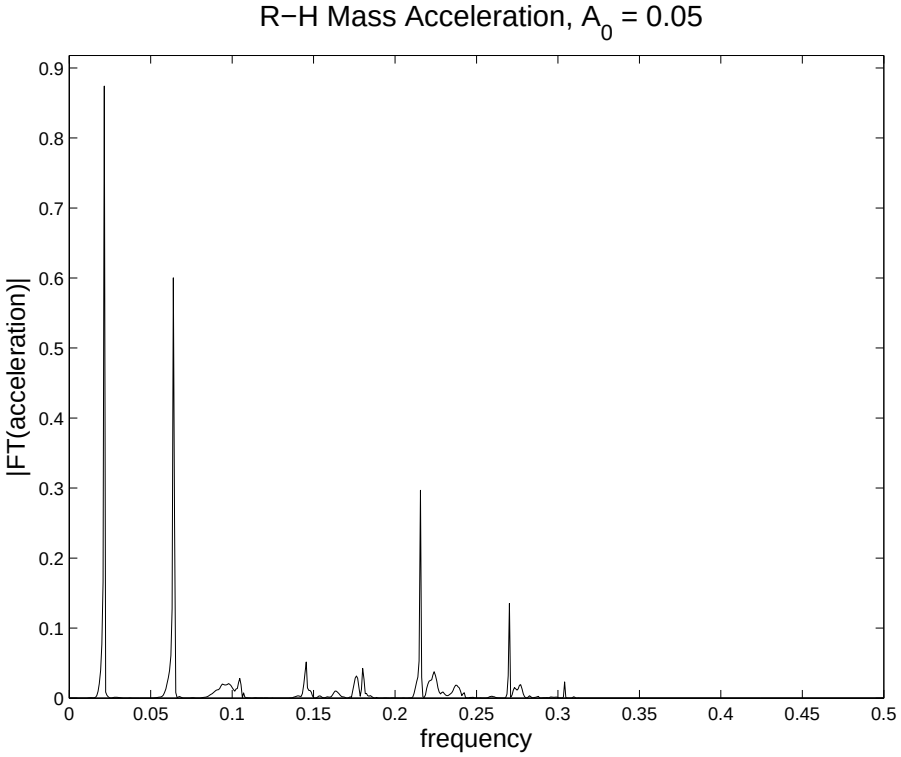

Figure 37. Macro-slip causes frequency responses of the structure that are well above that of the base excitation - which was tuned to the first resonance of the reference linear system. Shown here is the magnitude of the Fourier transform (MFT) of acclera-tion.

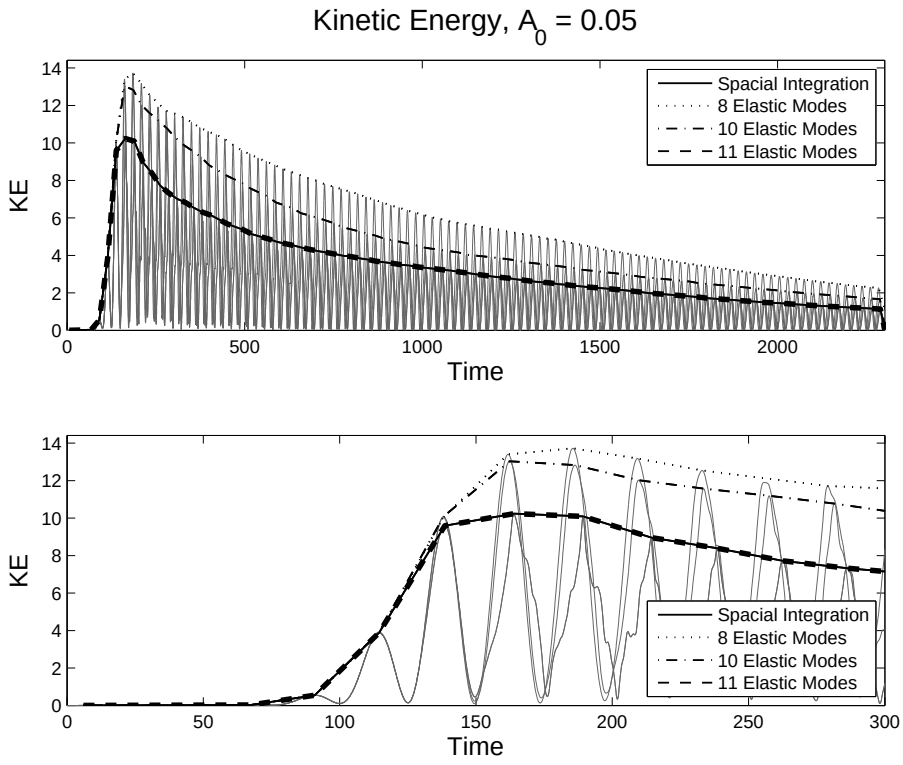

Figure 38. The Galerkin solution employing eigenmodes of the reference linear system generates a very poor approximation for the kinetic energy of the jointed system subject to a large amplitude impulse.

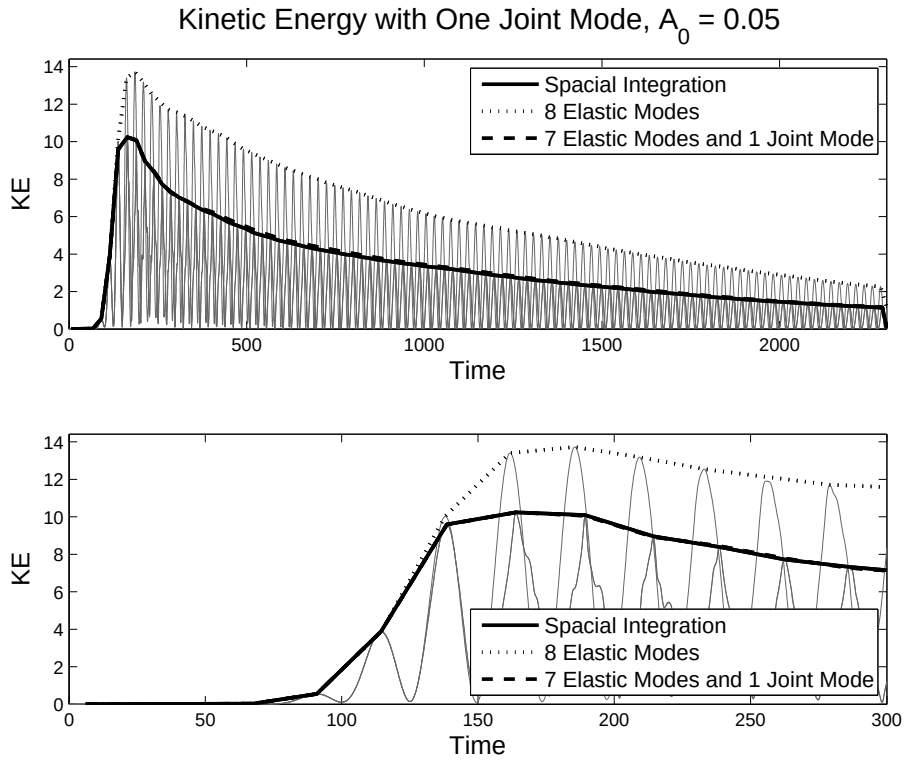

Figure 39. The Galerkin solution employing seven eigenmodes of the reference linear system augmented by one joint mode generates approximation for the kinetic energy of the jointed system subject to a large amplitude impulse. A large number of elastic modes are necessary to capture the high frequency response of the systems. The necessity of including the joint mode is illustrated by comparision to the prediction resulting from use of eight elastic modes.

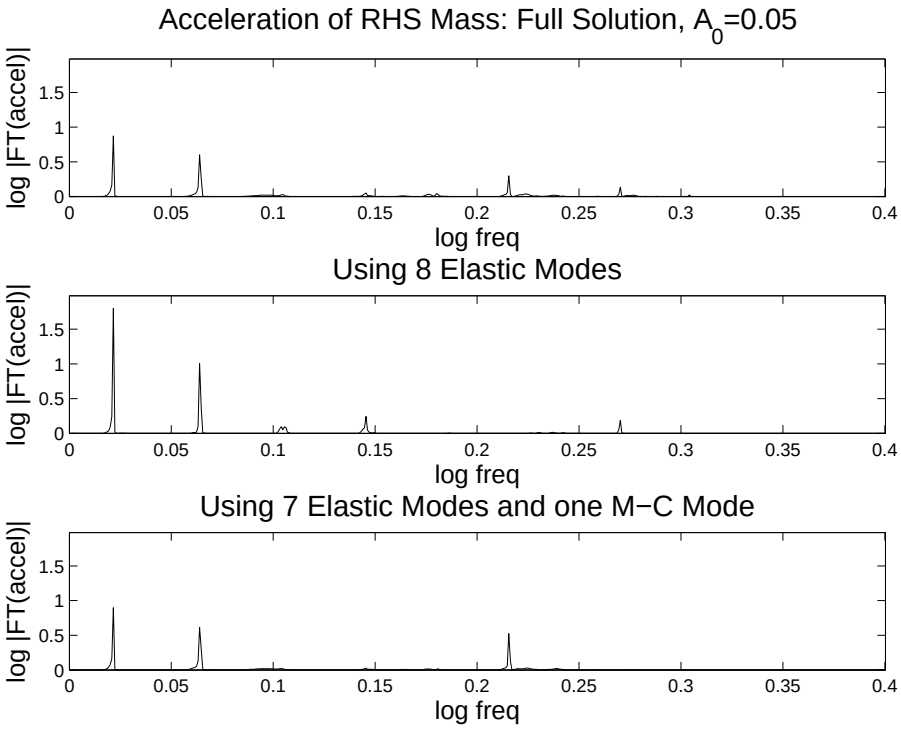

Figure 40. Comparison of the Fourier tranform magnitudes of the acceleration of the right most mass for the full spatial solution and the two reduced order solutions illustrates how resolution of joint kinematics is necessary to capture the energy shift from low frequencies to high. Shown here is the magnitude of the Fourier transform (MFT) of accleration.

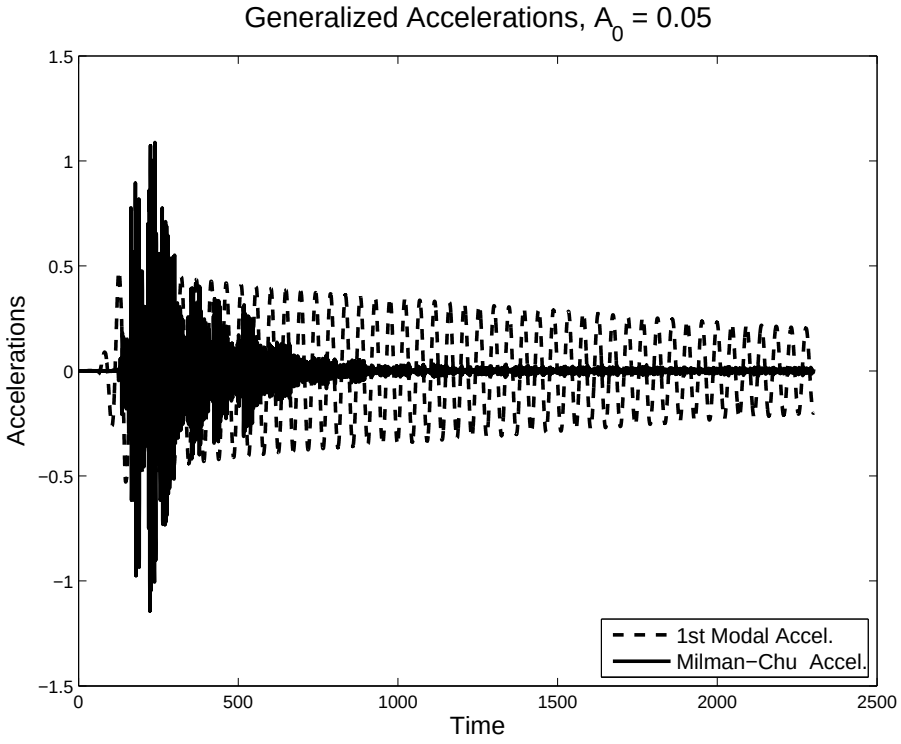

Figure 41. In this problem of macro-slip the generalized acceleration of the joint coordinate is no longer small.

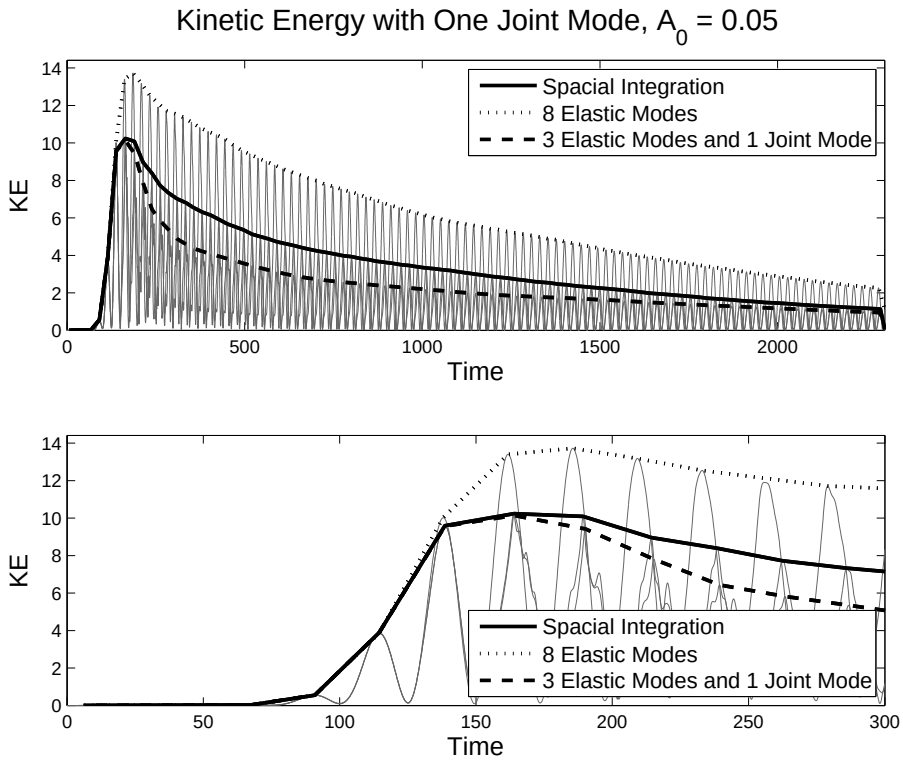

Figure 42. A "ruthlessly reduced" analysis using only three elastic eigenmodes and one joint mode results in noticable error in the kinetic energy, but substantially less error than an analysis using twice the number of elastic eigenmodes and no joint mode.

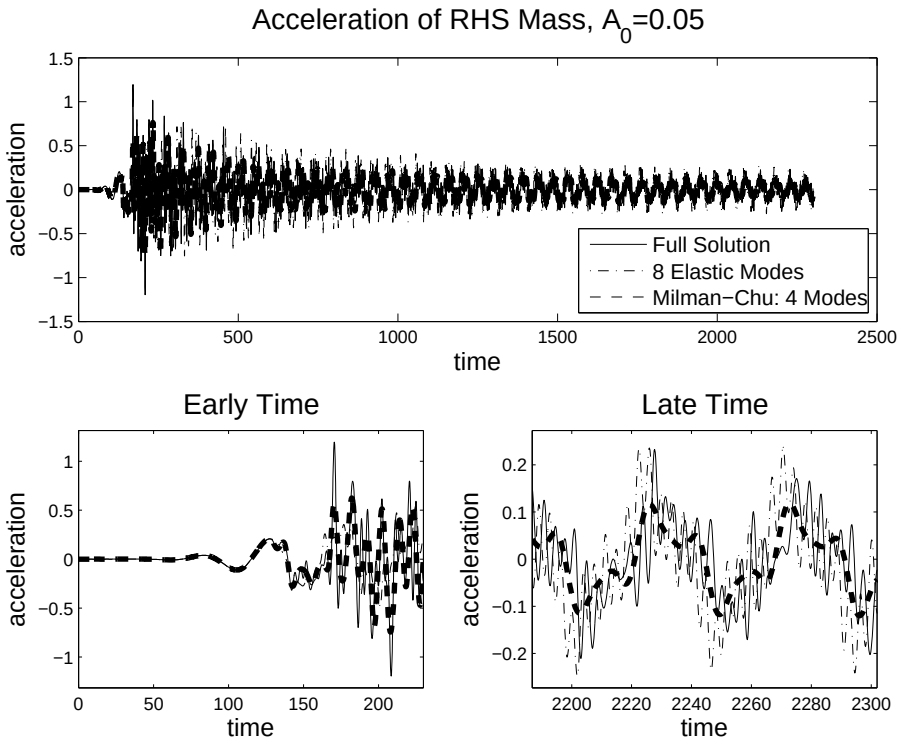

Figure 43. A "ruthlessly reduced" analysis using only three elastic eigenmodes and one joint mode results results in accelerations of the right most mass that have the appearance of a low-pass filter of the full spatial solution.

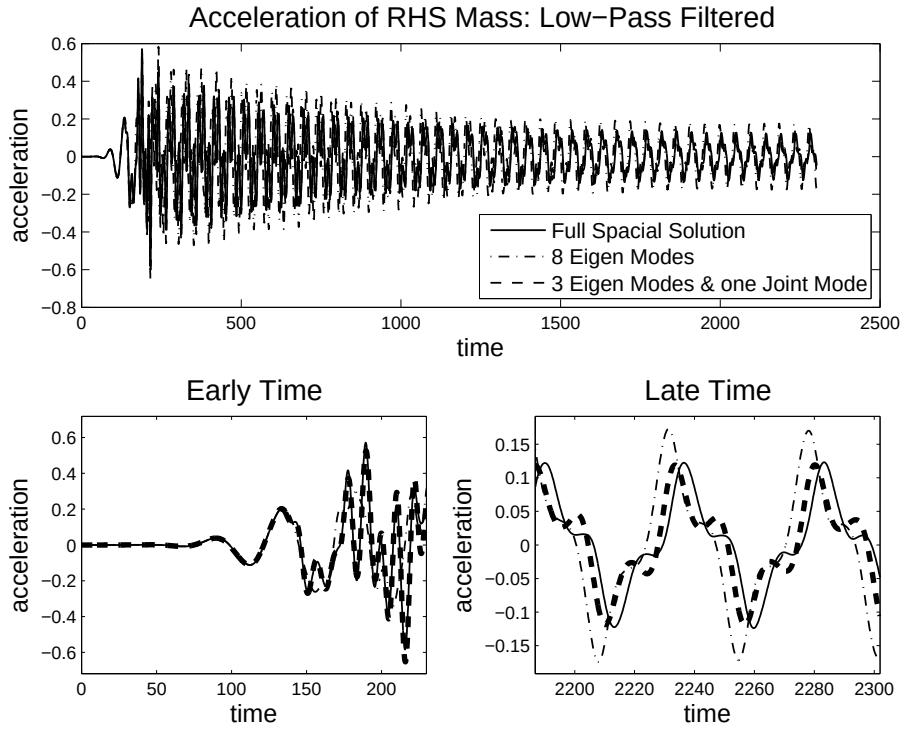

Figure 44. When the "ruthlessly reduced" analysis using only three elastic eigenmodes and one joint mode and the full spatial solution are seen through a low pass filter, they appear very similar.

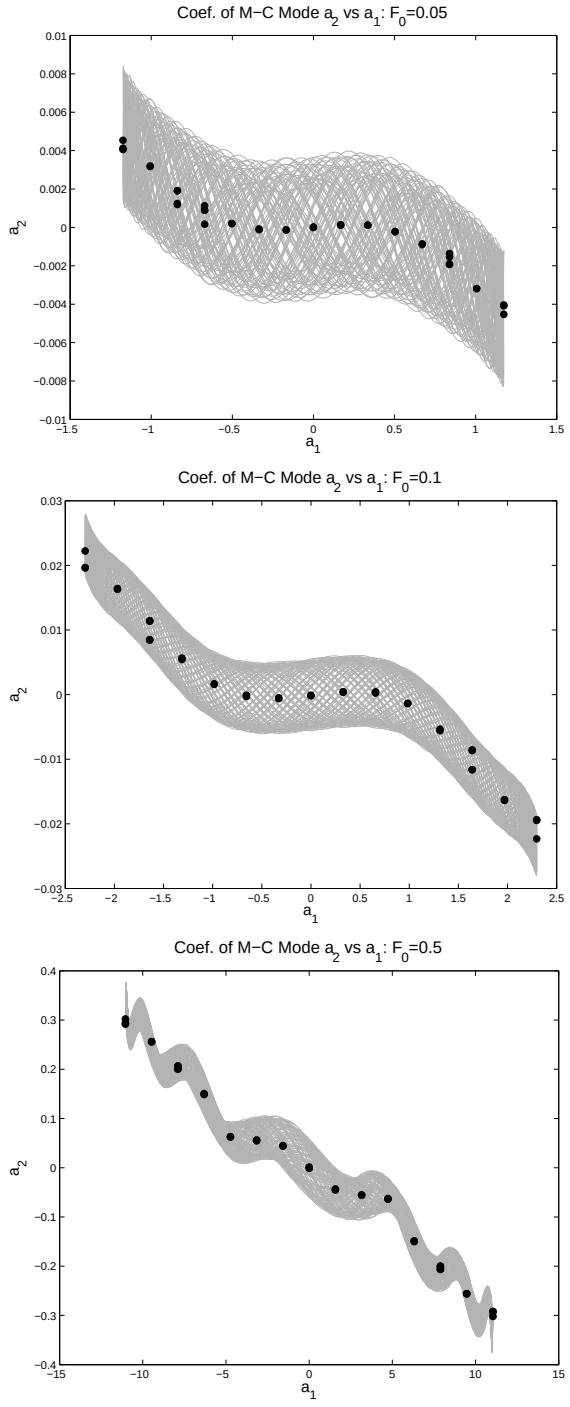

Figure A-1. When the coefficient for the first generalized coordinate (Milman-Chu) is plotted against the first, clouds (gray) associated with higher frequency result. When that the phase space $(a_1, \dot{a}_1)$ is distributed into bins and the values of a_2 in each bin in averaged, the points shown in dark squares results. The lack of scatter in these dots indicated the absense of velocity dependence - as it should.

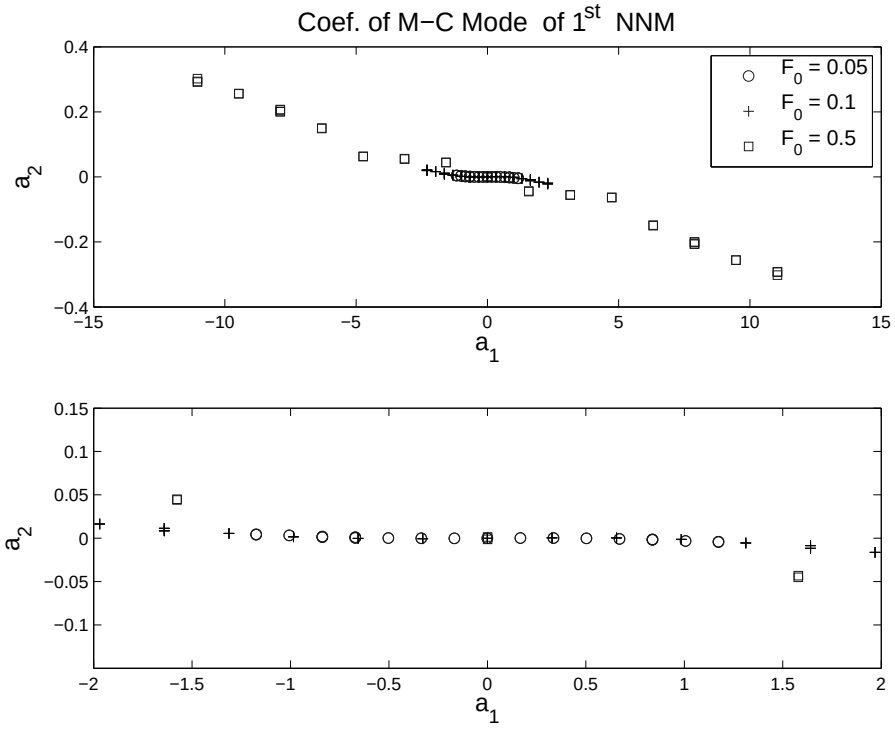

Figure A-2. When averaged mapping of the coefficient for the second generalized coordinate (Milman-Chu) against the first we see a pattern suggestive of the existance of a nonlinear normal mode.

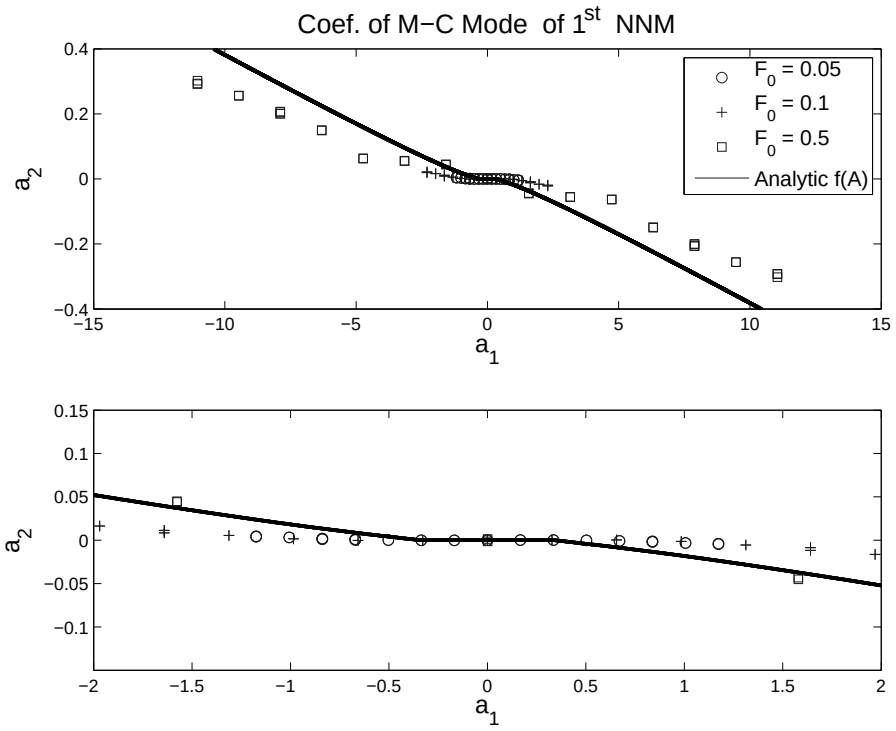

Figure A-3. When one assumes that a nonlinear normal mode exists and can be represened by the first eigenmode and a Milman-Chu mode, energy methods permit the estimation of the dependece of the second generalized coordinate as a function of the first.

DISTRIBUTION:

1 Professor Thomas Burton
Mechanical Engineering Department
New Mexico State University
PO Box 30001 MSC 3450
Las Cruces, NM, 88003

1 Professor Jerry Griffin
Department of Mechanical Engineering
Carnegie Mellon University
Pittsburgh, PA 15213

1 Professor Lawrence Bergman
306 Talbot Lab
104 S. Wright St.
University of Illinois
Urbana, IL 61801

1 Professor Daniel J. Inman
315 NEB
Mechanical Engineering
Virginia Polytechnic and State University
Blacksburg, VA 24061-0238

1 MS 0372
Bishop, Joseph E. , 1525

1 MS 0372
Jung, Joseph , 1525

1 MS 0372
Longcope Jr, D.B. , 1524

1 MS 0372
Pott, John , 1524

1 MS 0380
Alvin, Kenneth F. , 1542

1 MS 0380
Morgan, Harold S. , 1540

1 MS 0380
Reese, Garth M. , 1542

1 MS 0553
Smallwood, David O. , 1523

1 MS 0555
Gregory, Danny Lynn , 1521

1 MS 0555
Larkin, Paul A. , 1521

1 MS 0555
May, Rodney A. , 1522

1 MS 0555
Stasiunas, Eric Carl , 1521

1 MS 0557
Allen, Matthew Scott , 1526

1 MS 0557
Carne, Thomas G. , 1525

1 MS 0557
Griffith, Daniel , 1523

1 MS 0557
Mayes, Randall L. , 1521

1 MS 0557
O'Gorman, Christian , 1521

1 MS 0557
Resor, Brian R. , 1521

1 MS 0557
Rogillio, Brendan R. , 1521

10 MS 0557
Segalman, Daniel J. , 1525

1 MS 0557
Simmermacher, T. W. , 1523

1 MS 0825
Barone, Matthew F. , 1515

1 MS 0834
Hopkins, Matthew , 1514

1 MS 0847
Babuska, Vit , 1525

1 MS 0847
Baca, Thomas J. , 1523

1 MS 0847
Bitsie, Fernando , 1523

1 MS 0847
Dohrmann, Clark R. , 1523

1 MS 0847
Field Jr., Richard V. , 1526

1 MS 0847
Fulcher, Clay W. G. , 1526

1 MS 0847
Holzmann, Wil A. , 1523

1 MS 0847
Kmetyk, Lubomyra N. , 1527

1 MS 0847
Miller, A. Keith , 1523

1 MS 0847
Redmond, James M. , 1526

1 MS0557
Clauss, David B. , 1521

1 MS 0847
Rouse, Jerry W. , 1526

1 MS 0847
Starr, Michael J. , 1526

1 MS 0847
Tipton, D. Gregory , 1523

1 MS 0847
Wilson, Peter J. , 1520

1 MS 1070
Epp, David S. , 1526

1 MS 1070
Massad, Jordan E. , 1526

1 MS 1070
Sumali, Hartono , 1526

1 MS 1110
Lehoucq, Richard , 1414

2 MS 9018
Central Technical Files, 8944

2 MS 0899
Technical Library, 4536

1 MS 0123
D. Chavez, LDRD Office, 1011